Daniela Kirchmeyr, BSc

Cortical activity during motor execution and motor imagery of a hand grip exercise: A functional near infrared spectroscopy study

MASTER'S THESIS

to achieve the university degree of

Diplom-Ingenieurin

Master's degree programme: Biomedical Engineering

submitted to

Graz University of Technology

Supervisor

Ass.Prof. Mag.rer.nat. Dr.phil. Selina Christin Wriessnegger

Institute of Neural Engineering

Graz, October 2016

AFFIDAVIT

I declare that I have authored this thesis independently, that I have not used other than the declared sources/resources, and that I have explicitly indicated all material which has been quoted either literally or by content from the sources used. The text document uploaded to TUGRAZonline is identical to the present master's thesis.

3.10.2016
Date

Daniela Kirchmayr
Signature

Acknowledgments

I would like to use this opportunity to express my gratitude to all the people who supported me during the work of this thesis.

First of all, I want to thank my supervisor, Ass.Prof. Mag.rer.nat. Dr.phil. Selina Wriessnegger, who always took the time to answer my questions, provided good feedback and found possible solutions, whenever problems showed up.

Furthermore, I would like to thank Dipl.-Ing. Dr.techn. BSc Günther Bauernfeind, who suggested this topic and always offered his assistance during the first few months. Additionally, I want to thank all the people at the Institute of Neural Engineering, who always offered help and provided good input.

Finally, I would like to thank my parents, my brothers, friends and colleagues, for their support and encouragement during my studies.

Abstract

The aim of this thesis was to gain more knowledge about the haemodynamic response to motor execution and motor imagery by using functional near-infrared spectroscopy (fNIRS). On this account, the haemodynamic signal courses of thirteen subjects were measured and compared within five regions of interest (ROIs) related to the motor cortex. The conditions included motor execution and kinesthetic motor imagery of a hand grip exercise with two different predefined hand grip strengths. After a visual inspection of the signal quality, physiological artifacts were removed by applying a transfer function model on the raw signals. The analysis of the cleaned data revealed higher activation for motor execution than for motor imagery for both hand grip strengths. Additionally, a peak latency difference between motor execution and motor imagery was observed for oxy-Hb, independent of the used grip strength. According to the statistical analysis, no differences in the amount of activation for the different grip strengths were present. However, a difference concerning an oxygenation delay in case of the lower grip strength, if compared to the higher grip strength, during the motor execution condition was observable. The findings of this thesis are a first step in order to use a hand grip exercise with MI and ME and different grip strengths in stroke rehabilitation and assess the training progress by means of fNIRS.

Keywords: functional near-infrared spectroscopy, motor imagery, motor execution, haemodynamic signal changes, cortical activation

Kurzfassung

Das Ziel dieser Arbeit war es, mit Hilfe von funktioneller Nah-Infrarot Spektroskopie (fNIRS) mehr Kenntnisse über die hämodynamische Antwort auf Bewegungsvorstellung und Bewegungsausführung zu erlangen. Aus diesem Grund wurden die hämodynamischen Signalverläufe in fünf Bereichen des motorischen Kortex von 13 Probanden während vier verschiedenen Aufgaben verglichen. Diese beinhalteten Bewegungsvorstellung und Bewegungsdurchführung einer Handgreifbewegung, welche mit zwei verschiedenen Kraftstufen durchgeführt bzw. vorgestellt wurden. Nach der visuellen Inspektion der Signalqualität wurde ein Transfer-Funktions Modell auf die Rohsignale angewandt, um physiologische Artefakte zu reduzieren. Die Analyse der bereinigten Daten ergab eine stärkere Aktivierung für die Bewegungsdurchführung im Vergleich zur Bewegungsvorstellung. Auch eine Latenzverschiebung der Maxima von oxy-Hb bei Bewegungsvorstellung gegenüber der Bewegungsdurchführung war präsent. Diese beiden Beobachtungen waren unabhängig vom verwendeten Kraftaufwand. Die statistischen Analysen wiesen keine signifikaten Resultate auf, jedoch konnte eine Verschiebung der Oxygenierung in den Zeitverläufen der hämodynamischen Antwort bei Bewegungsdurchführung zwischen den beiden Kraftstufen beobachtet werden. Die gewonnenen Erkenntnisse dieser Arbeit sind ein erster Schritt, um eine Handgreifbewegung bzw. -vorstellung mit verschiedenen Kräften im Zuge der Schlaganfall-Rehabilitation einzusetzen und die Bewertung des Trainingserfolges mithilfe der fNIRS durchzuführen.

Schlüsselwörter: funktionelle Nah-Infrarot Spektroskopie, Bewegungsvorstellung, Bewegungsdurchführung, hämodynamische Signalverläufe, kortikale Aktivierung

Contents

List of Figures

List of Tables

Symbols, Abbreviations

Abbreviation	Meaning
fNIRS	functional near-infrared spectroscopy
oxy-Hb	oxygenated hemoglobin
deoxy-Hb	deoxygenated hemoglobin
$CMRO_2$	cerebral metabolic rate of oxygenation
CBF	cerebral blood flow
CBV	cerebral blood volume
ME	motor execution
MI	motor imagery
MGS	maximum grip strength
PFC	prefrontal cortex
pre-SMA	pre-supplementary motor area
SMA	supplementary motor area
PMC	premotor cortex
SMC	sensorimotor cortex

1 Introduction

1.1 Motivation

In 2011, 25.000 people in Austria suffered from stroke according to the latest report by the Austrian Federal Ministry of Health. 80% of these cases were ischaemic strokes. The incidence rate for ischaemic strokes is higher for older than for younger people. This is supported by the fact that 67% of all cases in 2011 occurred to people over the age of 69.

A stroke is one of the most frequent causes of death in Austria. In 2011, 1.7% of all deaths were attributed to stroke. Although the mortality rate has constantly decreased every year since 2003, the incidence rate is increasing steadily every year since 2008, both for men and women. [12]

Two basic forms of strokes are known, ischaemic strokes and haemorrhagic strokes. In both cases, the reason for the occurrence of a stroke is an oxygen deficiency of the brain caused by a disturbance of the blood supply. This oxygen deficiency results in necrosis of the brain cells. The magnitude of such a necrosis is determined by the duration of the circulatory disorder. The blockage of the blood flow to a certain brain region due to blood clots is called an ischaemic stroke, whereas the leaking or rupture of a blood vessel in the brain causes a haemorrhagic stroke. [36]

The results of the brain cell damages are very often lasting disability. Such disabilities can be speech disorders (dysphagia), visual disturbances, cognitive deficiencies and motor impairments. According to *Langhorne et al.*, 80% of the disabilities caused by stroke are motor impairments, which include hemiparesis, incoordination and spasticity [25, 37]. Possible causes of such an impairment are an injury to the motor cortex, the premotor cortex, motor tracts or associated pathways in the cerebrum or cerebellum [26].

The approximate locations of the motor related regions, i.e. the prefrontal cortex (PFC), the pre-supplementary motor area (pre-SMA), the supplementary motor area (SMA), the motor cortex and the premotor cortex (PMC), are illustrated in figure 1.1. In NIRS studies, the motor cortex and the sensory area are often treated as a single unit, the sensorimotor cortex (SMC) [17].

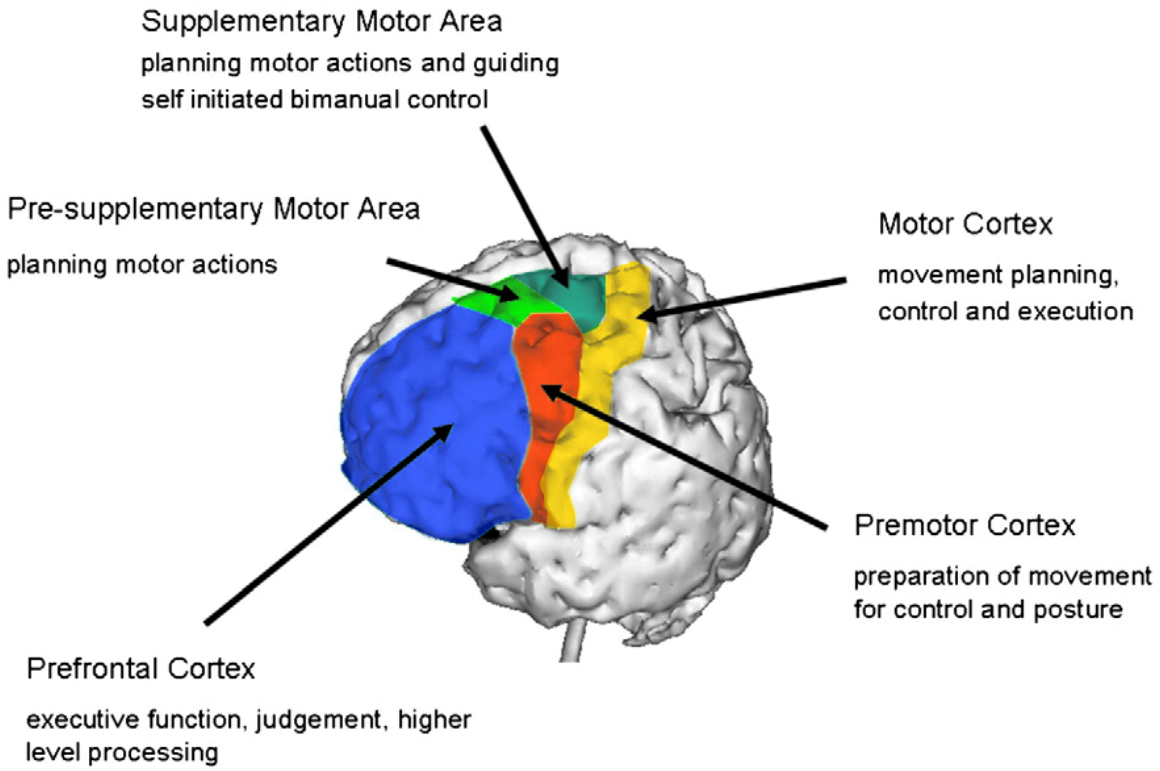

Figure 1.1: Depiction of the approximate locations of each of the motor related regions in the human cerebral cortex on a 3D anatomical MRI image (modified from [27])

In the first months after a stroke incident, the recovery of motor function due to rehabilitation care is most rapid. This recovery slows down and reaches a plateau by 6 months post-stroke [14]. The standard motor rehabilitation therapy typically involves a mix of physical and occupational training exercises. The standard duration during which a patient receives motor rehabilitation is 6 months, depending on the degree of impairment [37].

In the course of a review by *Zimmermann-Schlatter et al.* the possible role of motor imagery (MI) in stroke rehabilitation was investigated. They concluded that MI has a positive effect on stroke patients, in addition to conventional therapy. [44]

Motor imagery can be described as mental rehearsal of voluntary movement, which most people are able to do [1]. During such a mental rehearsal, the same cortical areas are activated as in case of an actual motor preparation and execution according to the 'simulation hypothesis' [18].

Motor imagery can be performed in two different ways, either visual or kinesthetic. During a kinesthetic motor imagery, the focus is on the kinesthetic experience of a movement while avoiding muscle tension. Visual imagery on the other hand is the mental visualization of a video, in which the specific movement is executed. *Neuper et al.* compared theses two different types of imagery and observed stronger activation in motor-related areas during kinesthetic motor imagery [32].

Kinesthetic motor imagery has already been used to investigate the reorganization processes of the brain after a stroke. These reorganization processes are induced by the damaged brain in order to compensate for the motor deficits by extending the functional scope of the intact areas of the brain [5]. The ongoing reorganization has been proven to be in relation to the recovery of motor functions [37].

Such a reorganization is induced by spontaneous occurring mechanisms and processes, but also promoted by rehabilitation. To investigate this reorganization, human brain mapping technologies have already been used. The understanding of these cortical reorganization processes further offers the possibility of using human brain mapping technologies for the determination of the most appropriate rehabilitation approach individually for each patient. Additionally, the effect of the rehabilitation protocol can be monitored with objective informations. [37]

Approximately 50-60% of stroke patients still have some degree of motor impairment after completing a standard rehabilitation. Therefore, the knowledge that can be obtained about brain plasticity by fNIRS can prove to be very meaningful for a patient specific training protocol and monitoring, as well as for the development of new effective therapies [37].

In order to gain a better understanding of reorganization processes, it is necessary to comprehend the activation patterns of a healthy brain first. This consideration and the possibility of using a NIRS system as a brain mapping device led to the fundamental idea behind this thesis, to get a better understanding of the behaviour of the brain and thus help people with impairments caused by stroke.

One possibility for a rehabilitation training exercise is the performance of a hand grip task. This exercise can be used to objectively assess the training progress, because of the possibility to measure the used force of the hand grip. Another advantage of a hand grip exercise is the fact that the ability to perform a hand grip after a stroke returns earlier than single finger movements, and therefore can be used for training earlier after stroke [40]. For this reasons, this thesis used a hand grip exercise, whose strength was measured by the PABLO® sensor handle[1].

[1] `www.tyromotion.com/en/products/pablo/pablo`

Because of the additional effect of the kinesthetic approach regarding motor imagery tasks, both motor execution (ME) and motor imagery (MI) were examined. Additionally, the hand grip strength was performed with two different forces, in order to investigate the possibility of a dependence between the activation pattern and the grip strength.

1.2 Basics of near-infrared spectroscopy

There are several possible human brain mapping technologies. Functional magnetic resonance imaging (fMRI) is the most commonly used technique, but additionally functional near infrared spectroscopy (fNIRS) is also applicable. Due to the fact that the motor areas are in close proximity to the scalp tissue, fNIRS can be used to monitor the haemodynamic response to brain activation in these regions [27]. Additionally, fNIRS offers the advantages of being portable, relatively robust to motion artefacts and cost-efficient [23]. Although fNIRS has a limited penetration depth [34] and a lower spatial resolution [43] compared to fMRI, *Kato et al.* found that both fMRI and fNIRS allowed the study of recovery of motor function after stroke [23]. Therefore, fNIRS has the potential to become a useful tool in neurorehabilitation [23, 31].

In 1977, *Jöbsis* presented in a paper, that it is possible, to noninvasively monitor cerebral oxygenation through the intact scalp with near infrared light. Specifically, the light must be within a certain wavelength range, the so called optical window (wavelengths about 700 to 1300nm), to penetrate the scalp and reach the cortex. [20]

The near-infrared light penetrating the head interacts with the tissue in several ways, for example in form of scattering events, or absorption. Next to water and lipids, other biological chromophores which absorb light in the given spectral range are respiratory enzymes and hemoglobin [6]. Due to the fortunate fact that hemoglobin has different optical properties, depending on the oxidation state, it provides useful information of the changes in the metabolism.

Near infrared spectroscopy is an optical method that employs this change of optical properties in order to noninvasively monitor brain activation by irradiating the brain with near infrared light and measuring the absorption of two different chromophores. Using the principle of neurovascular coupling (see chapter 1.2.1), the measured absorption, or rather the regional changes of the concentrations of oxygenated hemoglobin (oxy-Hb) and deoxygenated hemoglobin (deoxy-Hb) inferred of the absorption, are used to draw a conclusion about the activation of the investigated region of the cerebral cortex. [20, 33]

There are three different measurement methods with NIRS, the continuous wave approach, time resolved spectroscopy and the frequency domain technique. The time resolved spectroscopy (TRS) utilizes short pulses of NIR laser light in order to measure the time it takes for the light to penetrate the tissue, and therefore record the pathlength of individual photons. Additionally, depth information is also available in the temporal profile by distinguishing between early photons and late photons (see figure 1.2).

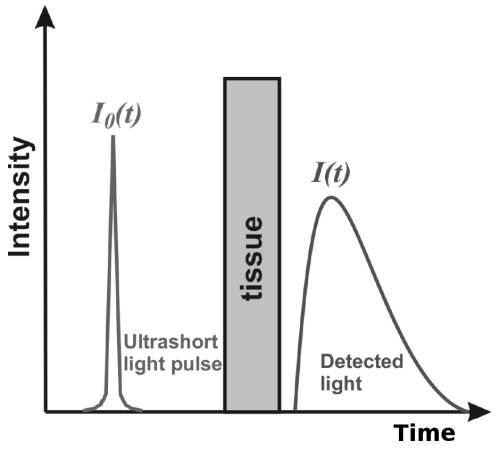

Figure 1.2: Schematic illustration of the temporal intensity profile for time resolved spectroscopy (modified from [2])

For the frequency domain technique (FDT), the intensity of the light is modulated with a frequency of 100 - 150 MHz. During the penetration of the tissue, both the intensity and the phase of the light are altered due to absorption and scattering effects, whereas the frequency stays the same. The temporal profile of this is illustrated in figure 1.3. The detected alterations can therafter be used to calculate the pathlength and the concentration changes of the chromophores.

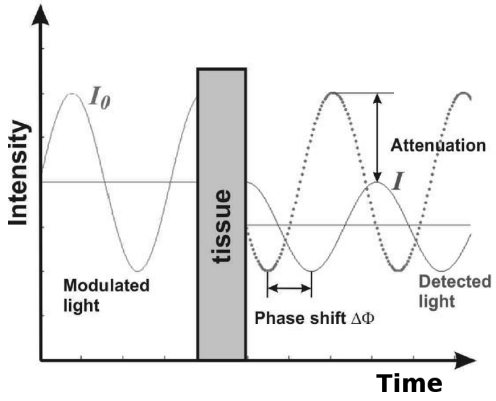

Figure 1.3: Schematic illustration of the temporal intensity profile for the frequency domain technique (modified from [2])

The continuous wave approach uses light with a constant intensity and measures the attenuation of the light after the penetration of the tissue (see figure 1.4). With this approach, the pathlength cannot be obtained. The advantage of the continuous wave approach is its simplicity, flexibility and high signal-to-noise ratio.

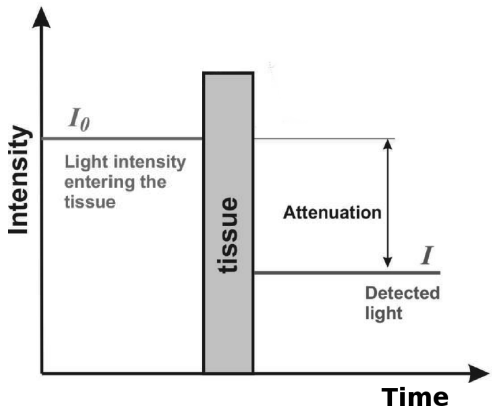

Figure 1.4: Schematic illustration of the temporal intensity profile for the continuous wave approach (modified from [2])

For further information on the time resolved spectroscopy and the frequency domain technique, the reader is referred to *Ferrari and Quaresima* [9], whereas the continuous wave approach is described in more detail in chapter 1.2.2, since it was used in this thesis.

1.2.1 Neurovascular coupling

The brain has a basic need for oxygen and glucose and every additional brain activity increases the consumption. This higher consumption leads to an increase of the cerebral metabolic rate of oxygenation ($CMRO_2$), the cerebral blood flow (CBF) and the cerebral blood volume (CBV). This interaction between the electrical neuronal activity of the brain, the $CMRO_2$, the CBF and the CBV is described by the term neurovascular coupling.

According to *Wolf et al.*, the three factors, $CMRO_2$, CBF and CBV, can change simultaneously during neuronal activation. An isolated change would result in the following alterations of [oxy-Hb] and [deoxy-Hb]:

- An increase of the $CMRO_2$ causes [oxy-Hb] to fall and [deoxy-Hb] to rise. (see figure 1.5) The reason for the increase of [deoxy-Hb] is the higher oxygen-consumption of the brain due to the neuronal activity.
- An increase of the CBF causes [oxy-Hb] to rise and [deoxy-Hb] to fall. (see figure 1.6) This increase of the CBF is a dominant factor, that can be easily measured, because it leads to a very high increase of [oxy-Hb].
- An increase of the CBV causes both [oxy-Hb] and [deoxy-Hb] to rise. (see figure 1.7)

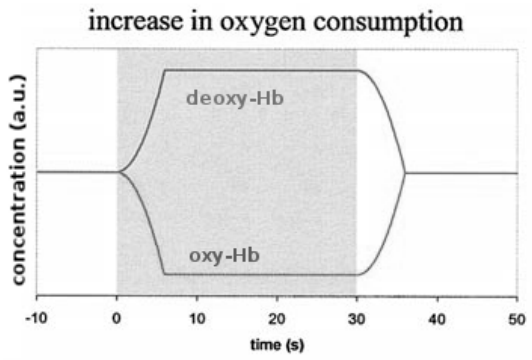

Figure 1.5: Changes of [oxy-Hb] and [deoxy-Hb] related to an isolated increase of the $CMRO_2$ (modified from [41])

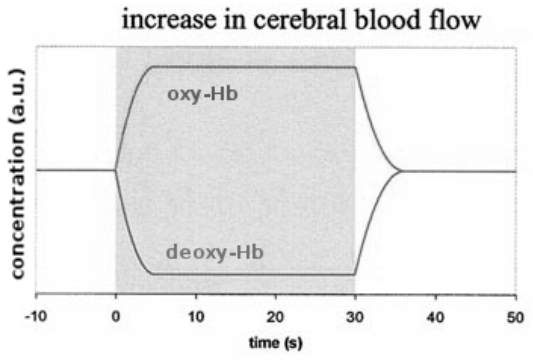

Figure 1.6: Changes of [oxy-Hb] and [deoxy-Hb] related to an isolated increase of the CBF (modified from [41])

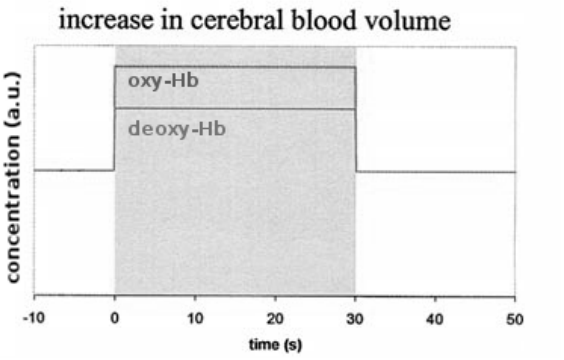

Figure 1.7: Changes of [oxy-Hb] and [deoxy-Hb] related to an isolated increase of the CBV (modified from [41])

After the cessation of the increased cortical activity, the concentrations return to their baseline values [41]. A combination of the three factors results in a typical course of [oxy-Hb] and [deoxy-Hb], which is depicted in figure 1.8. Due to the neurovascular coupling, and the knowledge of a typical course of [oxy-Hb] and [deoxy-Hb] during brain activation, it is possible to observe, whether a brain region shows neuronal activity by measuring the concentrations of oxy-Hb and deoxy-Hb over time.

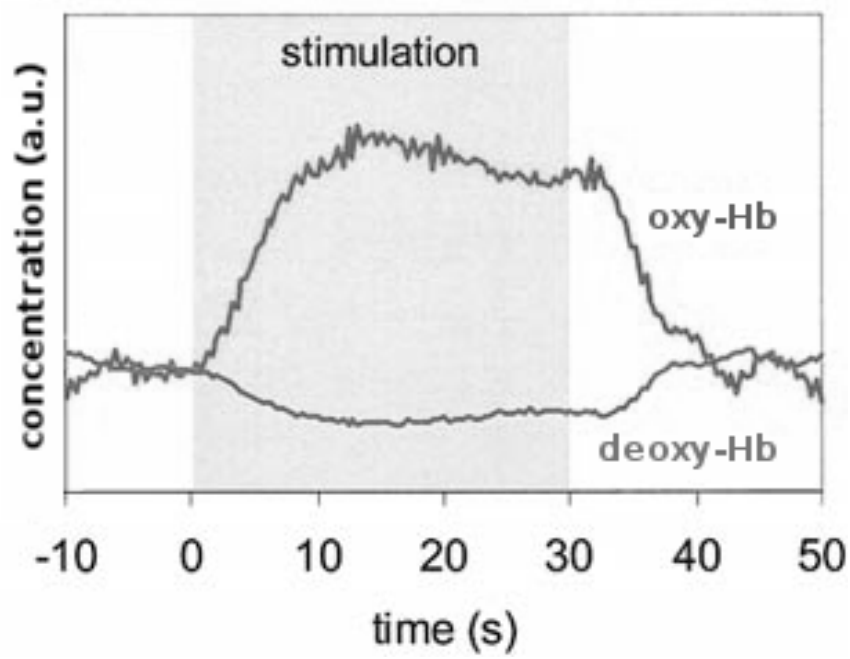

Figure 1.8: Typical course of [oxy-Hb] and [deoxy-Hb] during mental activation (modified from[41])

1.2.2 The continuous wave technique

The continuous wave approach is the most commonly used method for NIRS. The basic principle of this method is the radiation of the human scalp with light with a constant intensity by light emitting diodes. The attenuation of the light is then registered and used to calculate concentration changes of [oxy-Hb] and [deoxy-Hb] with the Beer-Lambert approach. By using a slightly modified version of this equation, scattering events are considered as well. Such scattering events occur during the transmission through the head. Therefore, the Beer-Lambert law is extended by a differential path length factor x, which takes into account, that the path length of each photon increases by the amount of scattering events, and by a term K describing the scattering losses, influenced by the geometry of the measurement. Since it can be postulated, that the geometry of the tissue does not change during a measurement, this scattering losses can be assumed as a constant. [7] The modified Beer-Lambert law is expressed in equation 1.1.

$$A = log(\frac{I_0}{I}) = \alpha \cdot c \cdot x \cdot d + K \tag{1.1}$$

A...attenuation, I_0...light intensity entering the tissue $[mW]$, I...light intensity exiting the tissue $[mW]$, α...specific extinction coefficient of the absorber $[l/(mol{\cdot}m)]$, c...concentration of the absorber $[mol/l]$, x...differential path length factor, d...geometrical distance between emitter and detector $[m]$, K...scattering losses

In order to calculate attenuation changes caused by a concentration change Δc, equation 1.2 can be used, which relies on the modified Beer-Lambert law.

$$\Delta A = \alpha \cdot \Delta c \cdot d \cdot x \tag{1.2}$$

In order to evaluate two chromophores, oxy-Hb and deoxy-Hb, two different wavelengths, λ_1 and λ_2 are necessary. By extending equation 1.2 for two wavelengths and two absorbers, it is possible to calculate the relative concentration changes of oxy-Hb and deoxy-Hb (see equation 1.3).

$$\begin{bmatrix} \Delta c_{deoxyHb} \\ \Delta c_{oxyHb} \end{bmatrix} = \begin{bmatrix} \alpha_{\lambda_{1,deoxyHb}} & \alpha_{\lambda_{1,oxyHb}} \\ \alpha_{\lambda_{2,deoxyHb}} & \alpha_{\lambda_{2,oxyHb}} \end{bmatrix}^{-1} \cdot \begin{bmatrix} \frac{\Delta A_{\lambda_1}}{x_{\lambda_1} \cdot d} \\ \frac{\Delta A_{\lambda_2}}{x_{\lambda_2} \cdot d} \end{bmatrix} \tag{1.3}$$

The different extinction coefficients for the two wavelengths and two chromophores are obtainable from [6].

1.3 Scientific background

Functional near infrared spectroscopy has already been used in a variety of studies concerning stroke rehabilitation. As mentioned before, *Kato et al.* compared fNIRS and fMRI in their study. They examined 6 stroke patients and 5 healthy control subjects during a hand movement task. Stroke patients exhibited activations at the contralateral motor cortex and at the ipsilateral motor cortex on affected hand movement. More precisely, these activations were observed at the SMC and the SMA. In case of the healthy control subjects, however, activations were obtained at the contralateral SMC and the SMA. These results were in agreement with both fMRI and NIRS. [23]

Miyai et al. also investigated the recovery after stroke by means of NIRS. During their measurement, eight stroke patients with hemiparetic gait had to walk on a treadmill. They focused on the SMC, the PMC and the SMA. They suggested an association between the improvement of asymmetry in SMC activation and enhanced PMC activation in the affected hemisphere with recovery after stroke. [31]

The results of a longitudinal NIRS study with near infrared spectroscopy done by *Takeda et al.* suggested that an increase in motor activation in the ipsilateral intact hemisphere within the first month after the stroke facilitates the motor functional recovery. They examined five ischemic stroke patients and five healthy subjects during the execution of a hand movement with optodes positioned on the scalp at the the primary sensorimotor areas. [39]

As mentioned before, motor imagery (MI) training may lead to an additional improvement in motor tasks after a stroke incident. For this reason, various studies have already been done on that matter. *Kaiser et al.* for example examined stroke recovery of 29 patients by measuring ERD and ERS patterns with EEG. [21]

An investigation done by *Holper and Wolf* focused on the differences of brain oxygenation patterns for different feedback conditions. They recorded fNIRS at the primary motor cortex in 15 healthy subjects while doing MI tasks and found that positive feedback produced higher activation compared to tasks without feedback. Even negative feedback showed higher activation than tasks without feedback, although not as high as for positive feedback. [15]

Wriessnegger et al. used functional near infrared spectroscopy to study the differences between movement execution and imagery. They examined 16 healthy subjects while doing a right and left hand tapping task and during kinesthetic movement imagery. Besides differences on the onset latencies of the oxygenation, they also found differences regarding the timing of lateralization processes between imagery and execution. [42]

Iso et al. studied the differences between motor execution and motor imagery during a tapping sequence. They found a significant interaction between task and hand in the SMC for oxy-Hb. The SMA and PMC showed a similar extent of activation for both motor execution and motor imagery. [17]

Leff et al. reviewed more than 80 studies regarding fNIRS measurements during motor tasks. Their aim was to summarize different studies and identify consistent outcomes. Their critical analysis yielded several limitations of previous studies and provided recommendations for future studies [27].

The methods used for the realization of this thesis are partially based on the recommendations by *Leff et al.*. Therefore, the main facts of their review are described in the following.

One of the consistent outcomes identified by *Leff et al.* concerned the haemodynamic response to motor stimulation. Independent of the type of motor stimulation and the study design, previous study results yielded a similar temporal pattern for the concentration changes of oxygenated hemoglobin (oxy-Hb) and deoxygenated hemoglobin (deoxy-Hb). According to this, an activation of the brain region can be described as a slow decrease in [deoxy-Hb] and a rapid increase in [oxy-Hb] of two- to threefold magnitude. [27, 28]

This is also consistent with the findings of *Wolf et al.*, concerning the typical course of [oxy-Hb] and [deoxy-Hb] during neurovascular coupling (described in chapter 1.2.1).

Regarding the temporal dynamics of the haemodynamic responses, a temporal offset of about 2 seconds was found in [deoxy-Hb] with respect to [oxy-Hb] [10]. The recovery of the haemodynamics has rarely been reported, but *Boden et al.* for example described a return to the baseline approximately 9 to 10 seconds after the end of the motor performance of both [oxy-Hb] and [deoxy-Hb] [4].

According to *Leff et al.*, the determination of an appropriate duration for the rest period in an experimental design is challenging, but 10 to 15 seconds should be satisfactory, depending on the stimulation protocol. [27]

One of the recommendations by *Leff et al.* concerned the kinematic motor performance. A variety of studies has already been done with measurements while performing a motor task. *Leff et al.* however mentioned, that the motor performance was not always objectively monitored or controlled. They recommended the usage of markers or kinematic outputs of motor performance such as EMG or force. [27]

In order to gain repeatable and comparable results, the strength of the hand grip was predefined and recorded in the course of this thesis by the PABLO® sensor handle[2].

[2] `www.tyromotion.com/en/products/pablo/pablo`

Another critical point mentioned by *Leff et al.* concerns the lack of uniformity regarding the positioning of the optodes. For this reason, in order to ensure replicable placement of the optodes, the Cz position of the international 10-20 system was used as a marker.

Hatakenaka et al. used anatomical MRI surface images to evaluate the anatomical location of the optodes. Dependent on the functional anatomy, the channels were then assigned to the corresponding regions of interest. [13] These definitions and locations were used in this thesis to specify the regions of interest, i.e. the left and right premotor cortex, the supplementary motor area, and the left and right sensorimotor cortex.

1.4 Analysis of haemodynamic data

Although many researches focus on fNIRS, no standard for the analysis of the haemodynamic data has yet been declared. *Leff et al.* proposed, that not only one haemoglobin species, which is considered as the best parameter of brain activation, should be examined, but oxy-Hb and deoxy-Hb. [27]

The first step of the typical approach for analysing the haemodynamic data consists of a segmentation of the fNIRS signal, for example by task onset. After that, all segments belonging to the same class of task are averaged. A comparison between the different tasks is then possible by means of statistical methods. Analysis of variance (ANOVA) or t-tests for example are used to examine, whether the differences between the averaged responses are statistically significant or not. This typical approach was also implemented in this thesis.

1.4.1 Reduction of systemic influences

Another recommendation by *Leff et al.* concerns the systemic physiological effects. In their opinion, physiological effects such as heart rate, respiration and third order BP waves (Mayer-Traube-Hering-waves) should be monitored and filtered from the measured signal [27], because they may influence and superimpose the measured fNIRS signal. Mayer-Traube-Hering-waves (MTH-waves) typically occur in a frequency range from 0.07 and 0.13 Hz [35]. The frequency of the respiration is typically in a range from 0.2 and 0.4 Hz, whereas for the pulse wave it is 1 to 2 Hz [3]. The power spectral density of an [oxy-Hb] signal, superimposed by these three systemic influences, can be seen in figure 1.9. Since the time constant of the activation response is 5-10s [8], especially respiration and MTH-waves may mask the haemodynamic response. Therefore, these influences have to be recorded and removed, in order to distinguish whether the signal is due to a brain activity or due to systemic influences.

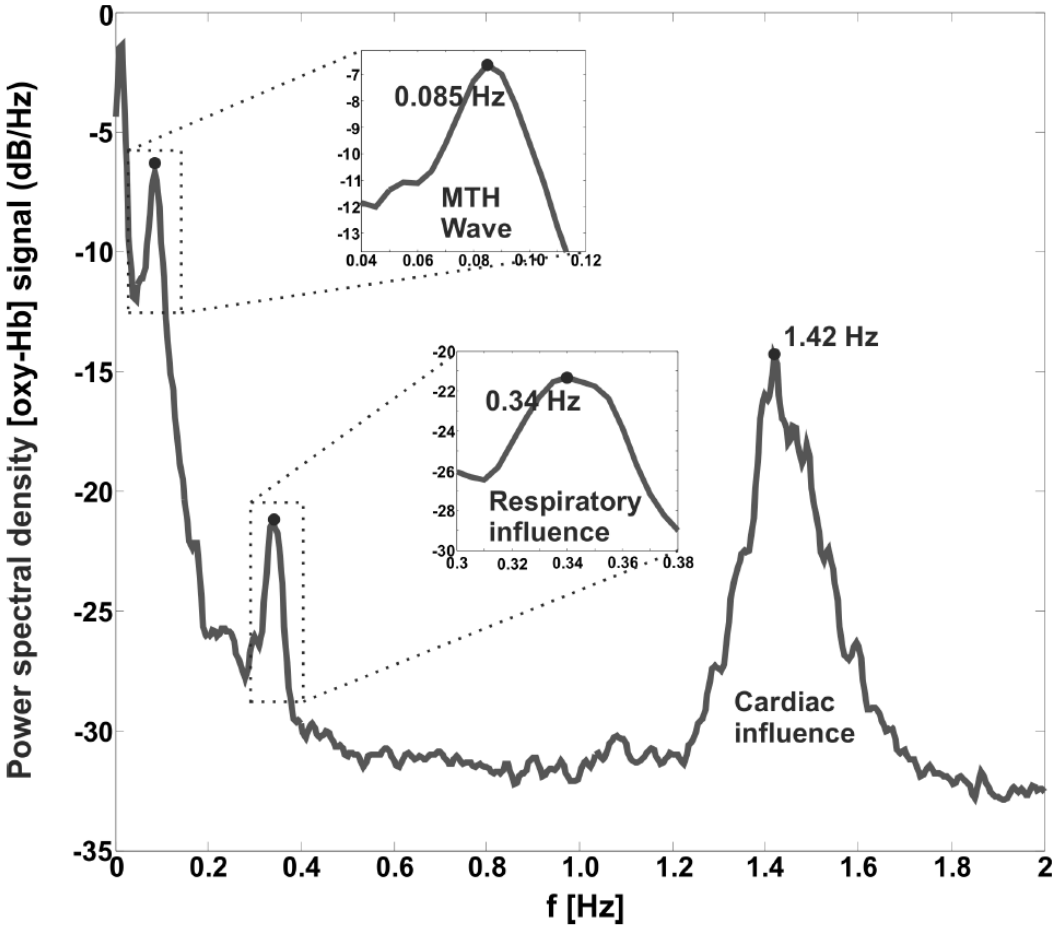

Figure 1.9: The power spectral density of an [oxy-Hb] signal of one subject, influenced by MTH-waves, respiration and heart rate (modified from [2])

A study by *Bauernfeind et al.* examined different signal processing approaches in order to find the best possibility to reduce physiological effects. They compared the impact of a common average reference (CAR) method, independent component analysis (ICA) and transfer function (TF) models on the signals.

Spatial filters like CAR are used in EEG analysis to reduce physiological noise. The idea behind the CAR method is that interfering signals are present in every channel, and can therefore be removed by subtracting the mean of all channels from each single channel for each time point. These method can be expressed with formula 1.4, with X being the raw signal, M the amount of channels and N the processed signal.

$$N_i[n] = X_i[n] - 1/M \sum_{j=1}^{M} X_j[n] \tag{1.4}$$

The ICA algorithm operates by finding a transformation matrix A, which represents the mixing of the independent sources (S) of artefacts. The resulting NIRS signal X can be expressed as shown in equation 1.5.

$$X = AS \tag{1.5}$$

TF models use measured physiological signals to remove these perturbances from the NIRS signal. This model can be expressed with equation 1.6, where N denotes the processed signal, X the raw signal, Y is the source of perturbation and the factors g_u are estimations of the impact of the source, calculated by minimizing the mean squared error.

$$N[n] = X[n] - \sum_{u=0}^{m} g_u Y[n-u] \tag{1.6}$$

A comparison of these three methods yielded a higher improvement of the contrast-to-noise ratio for the TF approach compared to ICA and CAR, both for [oxy-Hb] and for [deoxy-Hb] [3]. The TF model was also used in this thesis to reduce the influences of blood pressure and respiration.

1.5 Aim

The aim of this thesis was to investigate the haemodynamic response during motor imagery (MI) and motor execution (ME) using visually paced hand grip tasks with NIRS. These hand grip tasks had to be performed with two different grip strengths. Therefore, it was possible to examine, whether the activation patterns for ME and MI are dependent on the used strength. For the ME tasks, the force of the hand grip was measured by the PABLO® sensor handle and provided as visual feedback. During MI tasks, sham feedback was used. The analysis of the measured NIRS signals was performed with the described typical approach, including the TF model for artefact correction. Although some studies have already been done on ME and MI, to my knowledge, none of them measured the kinematic output of the motor performance or compared the concentration changes of two different grip strengths. Therefore, this thesis will provide new insights concerning differences between activation patterns of ME and MI, depending on the used grip strength.

2 Methods

2.1 Participants

Fourteen participants took part in this study, five of them female and nine male. The age of the participants was 25 ± 3. Thirteen of the participants were right-handed, one was left-handed, according to their own assessment. All participants had normal or corrected-to-normal vision, and no experience with motor imagery prior to this study.

2.2 Experimental procedure

The subjects were seated in a comfortable armchair in a dimmed cabin about 1.4 m in front of a monitor. After a detailed instruction they gave informed consent to participate in the study. Prior to the start of the measurement, the sensor handle was fixated on the right hand and the subjects had to grip it as forceful as possible for five times. The maximum grip strength of every subject was then calculated by averaging over these five measured values. A test run was presented on the monitor to allow the subjects getting familiar with the tasks and the the Pablo measuring and therapy device.

The measurement consisted of an alternation of runs with motor imagery (MI) and motor execution (ME). Every subject underwent six runs, three runs with ME, and three runs with MI, in randomized error. Irrespective of whether the condition was MI or ME, the experimental design of a run was the same. Every run consisted of 20 trials (10 trials with 20% of the maximum grip strength, 10 trials with 40% of the maximum grip strength), with a random alternation of the trials.

The timeline of a trial can be seen in figure 2.1. The start was indicated by the appearance of three white lines, encouraging the subjects to concentrate on the screen. After one second, one of the lines disappeared, the remaining line representing the hand grip strength that should be held or imagined during this trial. One second later the task performance began. After the 10 seconds of the task performance, the screen turned blank and the intertrial interval, with a duration randomly varying between 10 and 14 seconds, started.

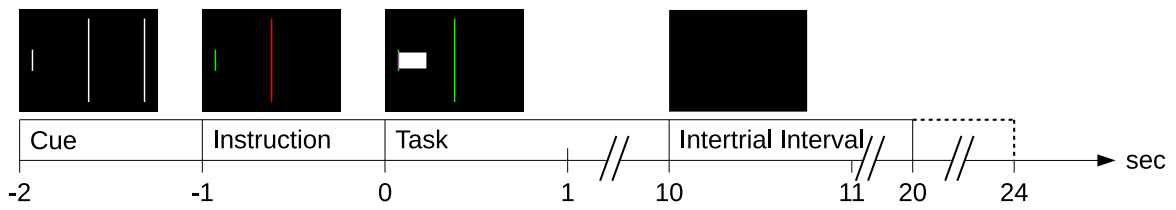

Figure 2.1: Schematic illustration of the experimental design

For the ME condition, the subjects were instructed to continuously perform a hand grip with a strength indicated by the line on the screen. To control the grip strength, the instantaneous gripping force measured by the Pablo Sensor handle was provided in form of a white feedback bar. This feedback bar appeared at the start of the task performance, indicating the current grip strength. The stronger a subject gripped the Pablo Sensor handle, the longer the feedback bar was. As the correct grip strength was indicated by a green line, the subjects were able to adjust their current grip strength according to the feedback bar.

The MI condition followed the same procedure, but instead of the execution of a hand grip, the imagination of a kinesthetic experience of such a hand grip had to be performed. Since *Holper and Wolf* found higher activation during MI tasks with feedback than without feedback [15], sham feedback was presented during the task performance. This sham feedback was presented in the same manner as it was done for the ME condition.

2.3 NIRS measurements

The fNIRS measurement was performed by using a continuous wave system (NIRScout 1624, NIRx Medizintechnik GmbH, Berlin, Germany). As with a continuous wave system it is not possible to measure the tissue optical pathlength, the scale unit of the system is the molar concentration multiplied with the unknown pathlength (mM mm). [9]

The used optode probeset consisted of 16 light emitters with two different wavelengths (760 nm and 850 nm) and 22 photo-detectors, resulting in a total amount of 61 channels (see figure 2.2). The inter-optode distance was 3 cm. In order to ensure a replicable placement of the optodes, detector 12 was placed at the position of Cz according to the international 10-20 system. The sample rate was 3.91 Hz.

For this channel configuration, five regions of interest (ROIs) were defined according to *Hatakenaka et al.*[13]. In figure 2.2 the ROIs are marked with dashed lines. The ROIs 1 and 3 cover the left and right premotor cortex (PMC), ROI 2 the supplementary motor area (SMA), and the ROIs 4 and 5 the left and right sensorimotor cortex (SMC). ROI 1 consisted of the channels 8, 15, 18 and 28, ROI 2 of the channels 17, 18, 19 and 20, ROI 3 of the channels 12, 19, 22 and 32, ROI 4 of the channels 28, 29, 30 and 31 and ROI 5 of the channels 32, 33, 34 and 35.

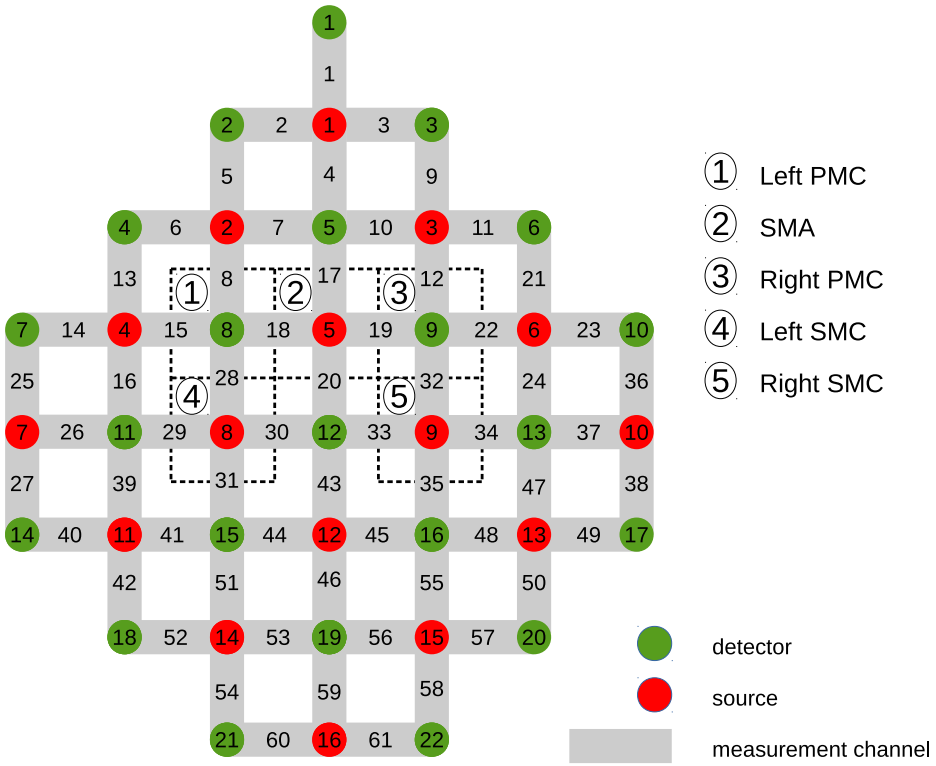

Figure 2.2: Channel configuration of the optode probeset:
16 light sources and 22 photo-detectors form 61 measurement channels

2.4 Physiological data acquisitions

Simultaneously with the fNIRS recording, physiological data, the electrocardiogram (ECG), the blood pressure and the respiration, was acquired. The ECG was recorded with electrodes placed on the thorax. For the recording of the respiration a respiratory sensor (Respiratory Effort Sensor, Pro-Tech Services, US) was used. Both ECG and respiration were obtained by a g.USBamp biosignal amplifier (Guger Technologies, Austria) with a sample rate of 255.99 Hz. The blood pressure was registered at the proximal limp of index or middle finger with the CNAP™ Monitor 500 (CNSystems Medizintechnik AG, Austria).

In order to measure the hand grip strenght, the PABLO® sensor handle (Tyromotion, Austria) was used, which is shown in figure 2.3. This device is able to measure a grip force up to 1000 N dynamically.[3] The PABLO® software tyroS version 3.0 offers the opportunity to transmit data via TCP connection, creating the possibility to receive it in MATLAB and present it as continuous feedback in the experimental paradigm, as mentioned in section 2.2.

[3]PABLO® Instruction Manual, Edited on March 16, 2015 (PABLO_PR3_Gebrauchsanweisung)

Figure 2.3: The PABLO® sensor handle

2.5 Data processing

For data processing MATLAB version R2012b was used. Baseline removal, i.e. a high pass filter with a cut-off frequency at 0.01 Hz, and low pass filtering (cut-off frequency at 0.8 Hz) were applied on the oxy-Hb and the deoxy-Hb signals. Since respiration with frequencies between 0.2 and 0.4 Hz, and 3rd order blood pressure waves (Mayer-Traube-Hering (MTF) waves, around 0.1 Hz [35]) superimpose the recorded NIRS signals, transfer function (TF) models were applied. Therefore, the recorded respiratory signal and the HR signals were band-pass filtered between 0.2 and 0.4 Hz, and 0.07 and 0.13 Hz, and downsampled to the sample rate of the NIRS signals, i.e. 3.91 Hz. By applying the transfer function model with these downsampled signals, it is possible to reduce the systemic influences. [3]

For each subject, the concentration changes of oxy-Hb and deoxy-Hb were averaged over each recorded trial per task. Both ME and MI were repeated three times with 10 trials per condition, therefore 30 data sets went in the calculation of the mean values for each subject. Additionally, a calculation of the concentration changes of every region of interest was performed by averaging over the signals of the four included channels, which are marked in figure 2.2. Artifacts and optode failures registered by visual inspection were discarded from all analysis.

2.6 Statistical analyses

Statistical analyses were performed on the maxima of the concentration changes of oxy-Hb and the maxima of the concentration changes of deoxy-Hb for each subject and each region of interest. In the following, the maximum values of the concentration changes of oxy-Hb and deoxy-Hb are denoted as max[oxy-Hb] and max[deoxy-Hb]. The time point of max[oxy-Hb] was defined for each subject individually by visual inspection. The corresponding max[deoxy-Hb] were then obtained in relation to the time point of max[oxy-Hb] $\pm$ 4 seconds. With these calculated parameters analyses of variance (ANOVA) and t-tests were realised separately by using RStudio Version 0.99.902.

First of all, a 2x2x5 ANOVA with repeated measurements was conducted. The ANOVA design included the factors *Task (ME and MI)*, *Force (20% and 40%)* and *ROI (left PMC, SMA, right PMC, left SMC, right SMC)*.

For a further investigation of the influence of the two different forces on the signal, paired-samples t-tests were also implemented using RStudio, comparing the maximum values of 40% with the maximum values of 20% of the MGS for every ROI, the two different conditions, and oxy-Hb and deoxy-Hb separately.

To evaluate observed lateralization differences, paired-samples t-tests comparing right and left SMC were conducted for every condition and oxy-Hb and deoxy-Hb separately.

3 Results

In tfhe following, the gained results in respect to the motor execution task (subsection 3.1), the motor imagery task (subsection 3.2), the observed latency differences between motor execution and motor imagery (subsection 3.3), the differences between the ROIs (subsection 3.4) and the topographic distributions (subsection 3.5) are described.

The main result was the difference of the maximum values between the two tasks, MI and ME. There was no statistically significant result regarding differences between the five defined ROIs. For the MI task a significant difference between 20% and 40% of the maximum grip strength (MGS) was found at the right PMC. Another difference regarding the two tasks was found in form of a delayed response in the imagery task. Additionally, ME with 20% of the MGS also showed a delayed response compared to ME with 40% of the MGS.

Due to technical problems, one subject was excluded from all calculations. Therefore, the measurements of 13 subjects went into further analysis. This analysis included a 2x2x5 ANOVA and several post-hoc tests, which are going to be presented in later chapters. The results of the 2x2x5 ANOVA with repeated measurements on the factors *Task (ME, MI)*, *Force (20%, 40% of the MGS)* and *ROI (left PMC, SMA, right PMC, left SMC, right SMC)*, and their interactions, are summarized in table 3.1. For oxy-Hb, the test revealed a significant main effect for the factor *Task* (F(1,12)=22.45, p=0.00048).

Table 3.1: Main results of the 2x2x5 ANOVA with repeated measurements

	oxy-Hb		**deoxy-Hb**	
ROI	F(4,48)=0.3556	p=0.83887	F(4,48)=0.7465	p=0.56520
Task	F(1,12)=22.4502	p=0.00048 ***	F(1,12)=0.0290	p=0.86755
Force	F(1,12)=0.2480	p=0.62751	F(1,12)=4.3239	p=0.05969
ROIxTask	F(4,48)=0.5146	p=0.72532	F(4,48)=0.4585	p=0.76576
ROIxForce	F(4,48)=2.1101	p=0.09404	F(4,48)=1.3816	p=0.25439
TaskxForce	F(1,12)=1.0225	p=0.33187	F(1,12)=0.2335	p=0.63762
ROIxTaskxForce	F(4,48)=0.8779	p=0.48423	F(4,48)=0.4604	p=0.76439

*** $p < 0.001$

In figure 3.1, the averaged concentration changes of oxy-Hb and deoxy-Hb are illustrated, comparing the four different tasks.

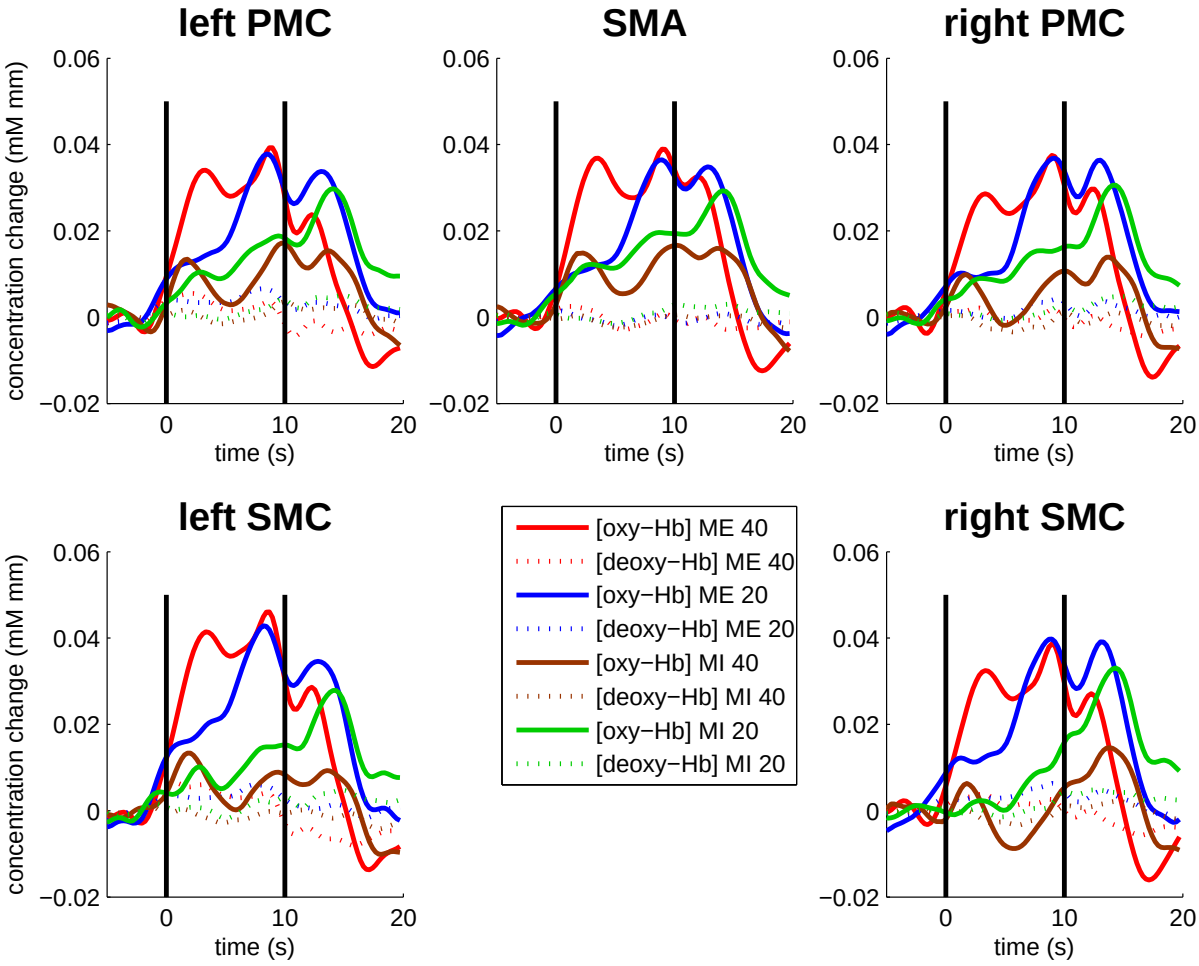

Figure 3.1: Mean concentration changes of oxy-Hb (solid lines) and deoxy-Hb (dotted lines) in the five ROIs for $ME_{40\%}$, $ME_{20\%}$, $MI_{40\%}$ and $MI_{20\%}$

In the following, motor execution tasks with 40% or 20% of the maximum grip strength (MGS) are denoted as $ME_{40\%}$ or $ME_{20\%}$ and motor imagery tasks with 40% or 20% of the MGS are denoted as $MI_{40\%}$ or $MI_{20\%}$ respectively. Furthermore, the mean concentration changes of oxygenated hemoglobin and deoxygenated hemoglobin, averaged over all trials of all subjects for the respective condition, are abbreviated as [oxy-Hb] and [deoxy-Hb].

3.1 Motor execution

In this section, the differences in brain activity between the two different grip strengths are described. Figure 3.2 depicts [oxy-Hb] and [deoxy-Hb] for each ROI during ME for 40% (black line) and 20% (grey line) of the MGS, averaged over 13 subjects. The two vertical lines are indicating the start point (t=0s) and end point (t=10s) of the task performance. These lines are used in every plot regarding the concentration changes over time.

By comparison, a latency difference between [oxy-Hb] for $ME_{40\%}$ and [oxy-Hb] for $ME_{20\%}$ is observable in every ROI. Although both rise at approximately the same time point, [oxy-Hb] for $ME_{40\%}$ reaches its first peak at an earlier point in time. Additionally, it is also levelled out earlier.

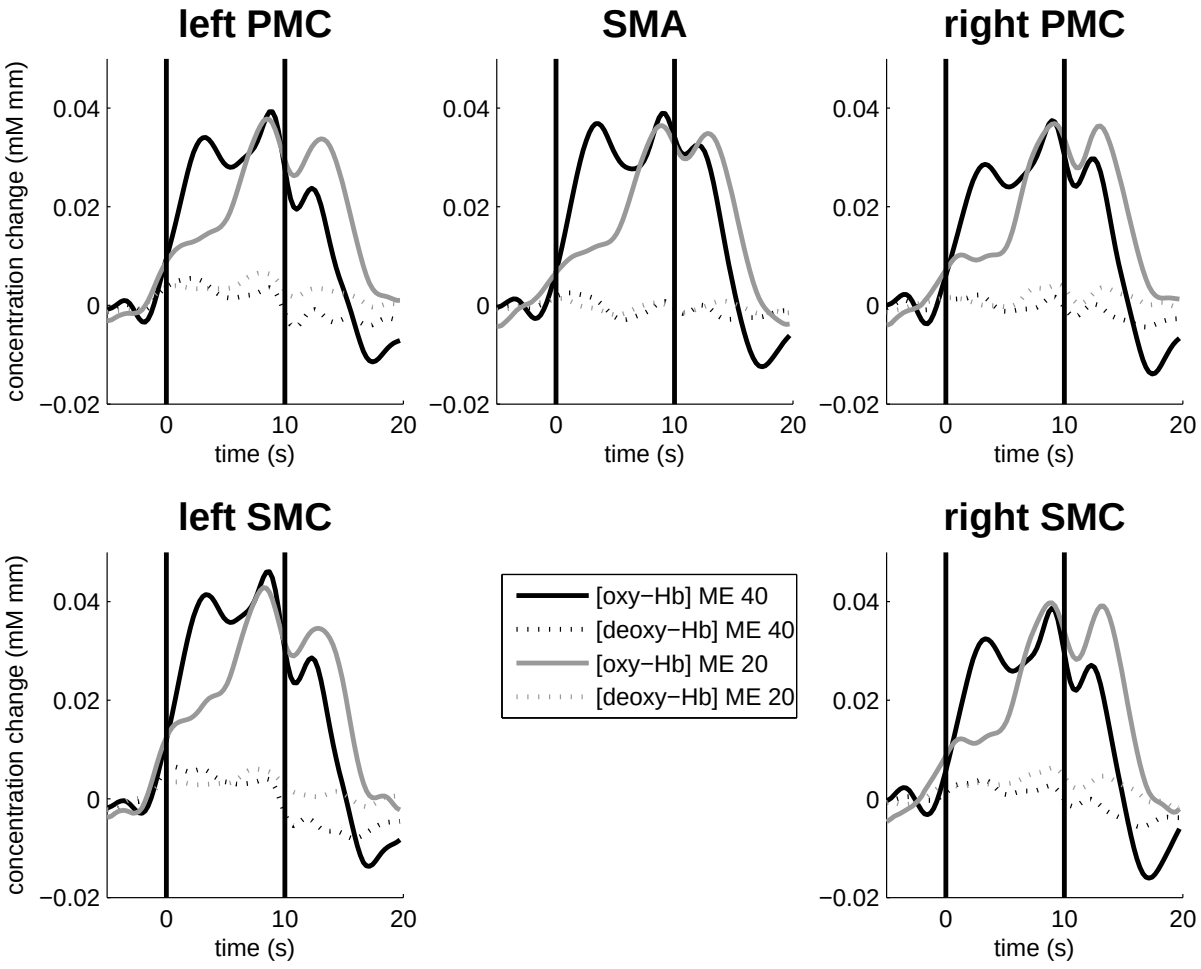

Figure 3.2: [oxy-Hb] (solid lines) and [deoxy-Hb] (dotted lines) in the five ROIs for $ME_{20\%}$ and $ME_{40\%}$

The maximum of [oxy-Hb] for $ME_{40\%}$ is slightly higher in the ROIs left SMC, left PMC and SMA than for $ME_{20\%}$, whereas for right PMC and right SMC it is approximately the same. The performed paired-samples t-test on [oxy-Hb], however, revealed no significant differences between the maximum values of $ME_{40\%}$ and $ME_{20\%}$ for any ROI. The same observation is made regarding [deoxy-Hb] (see table 3.2).

Table 3.2: Results of the paired-samples t-tests for ME

	oxy-Hb		**deoxy-Hb**	
ROI 1	t(12)=-0.3550	p=0.7288	t(12)=1.7787	p=0.1006
ROI 2	t(12)=-1.0340	p=0.3215	t(12)=-0.1244	p=0.9031
ROI 3	t(12)=-0.0948	p=0.9260	t(12)=1.6617	p=0.1224
ROI 4	t(12)=-0.4841	p=0.6371	t(12)=1.1725	p=0.2637
ROI 5	t(12)=0.3954	p=0.6995	t(12)=2.0866	p=0.0589

3.2 Motor imagery

Figure 3.3 illustrates [oxy-Hb] and [deoxy-Hb] during MI for each of the five ROIs. As observed for motor execution, [oxy-Hb] for $MI_{40\%}$ displays a faster rise than for $MI_{20\%}$, but instead of a successive climb to its maximum, the signal decreases again, before a second local maxima occurs. On the other hand [oxy-Hb] for $MI_{20\%}$ rises slowly but constantly to a peak approximately at second 15, which is definitely higher than the peak of [oxy-Hb] for $MI_{40\%}$.

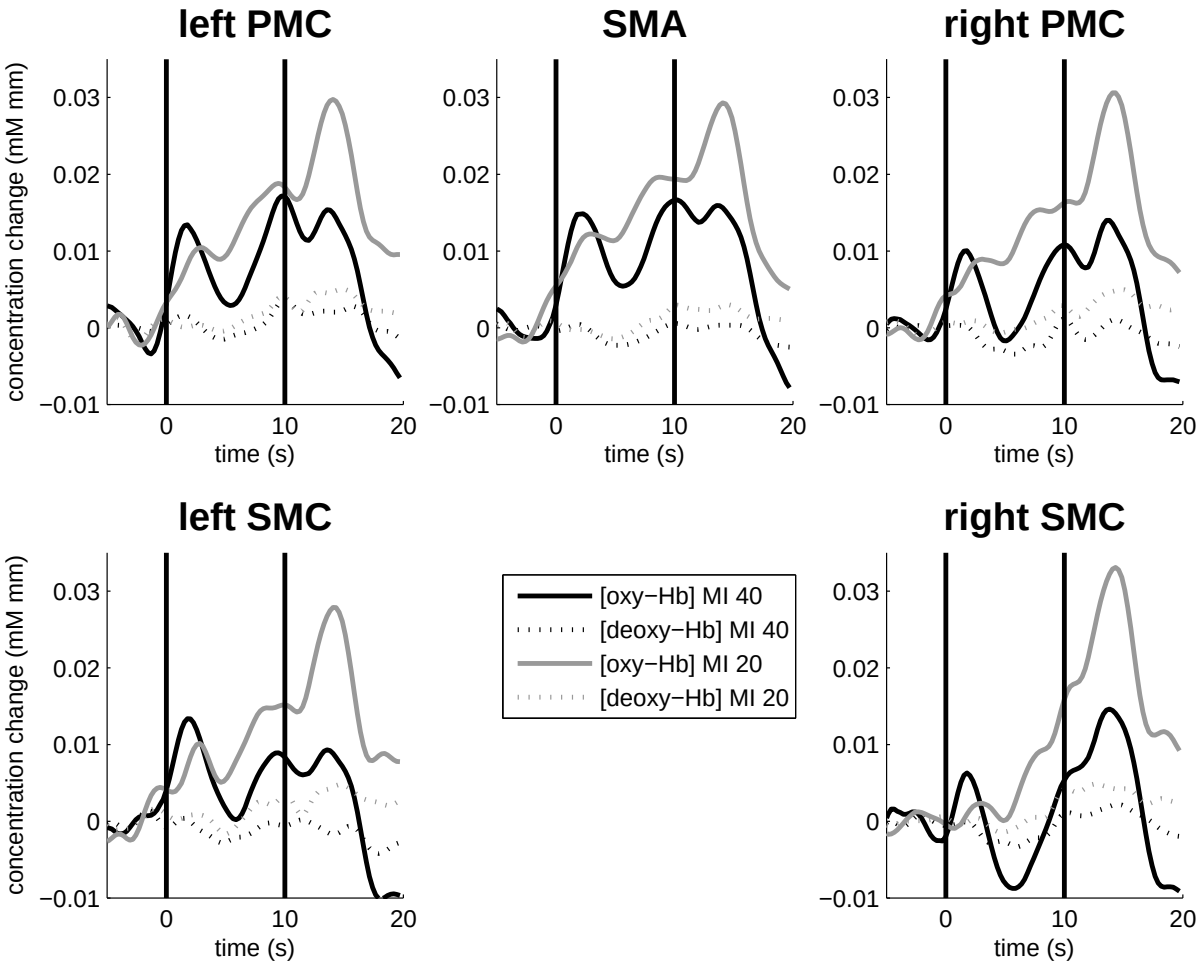

Figure 3.3: [oxy-Hb] (solid lines) and [deoxy-Hb] (dotted lines) in the five ROIs for $MI_{20\%}$ and $MI_{40\%}$

The results of the paired-samples t-test comparing the maximum values of $MI_{20\%}$ and $MI_{40\%}$ for each ROI are presented in table 3.3 for both oxy-Hb and deoxy-Hb. For the right PMC ROI, the paired-samples t-test reveals a significant difference between $MI_{20\%}$ and $MI_{40\%}$ (t(12)=2.6521, p=0.0211; see table 3.3). The calculated average of the maximum values for $MI_{40\%}$ is 0.0276 mM mm (SD=0.0230), and 0.0372 mM mm (SD=0.0259) for $MI_{20\%}$. For deoxy-Hb, no significant result is revealed (see table 3.3).

Table 3.3: Results of the paired-samples t-tests for MI

	oxy-Hb		**deoxy-Hb**	
ROI 1	t(12)=1.0726	p=0.3045	t(12)=1.3428	p=0.2042
ROI 2	t(12)=1.0253	p=0.3255	t(12)=1.1714	p=0.2642
ROI 3	t(12)=2.6521	p=0.0211*	t(12)=1.7901	p=0.0987
ROI 4	t(12)=0.7738	p=0.4540	t(12)=2.0842	p=0.0592
ROI 5	t(12)=1.1302	p=0.2805	t(12)=1.7594	p=0.1040

* $p < 0.05$

3.3 Latency differences between MI and ME

In figure 3.4, [oxy-Hb] and [deoxy-Hb] for the two different conditions are illustrated for each of the five ROIs. As can be seen in each of the five subgraphs, the oxy-Hb concentration changes for ME are definitely higher than that for MI, independent of the ROI. This was also confirmed by the 2x2x5 ANOVA test, that reveals a significant main effect for the factor *Task* ($F(1,12)=22.45$, $p=0.00048$; see table 3.1)

The oxygenation onset seems to be approximately the same for the four different conditions, but between ME and MI a peak latency difference can be observed. Whereas the averaged peak for ME is at second 9.2947 (SD=3.7934), it is at second 12.5005 (SD=3.8900) for MI.

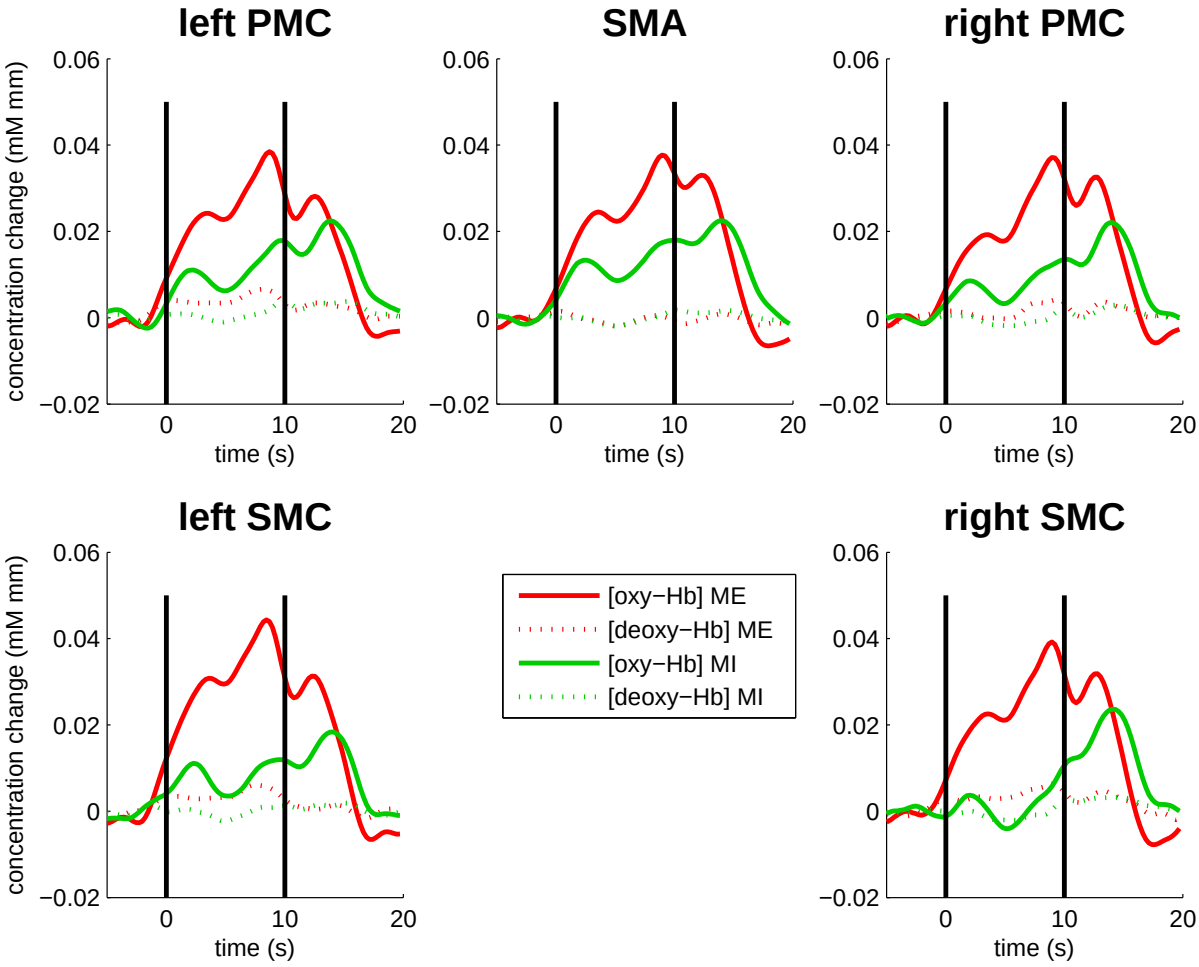

Figure 3.4: [oxy-Hb] (solid lines) and [deoxy-Hb] (dotted lines) in the five ROIs for ME and MI

3.4 Differences between ROIs

In figure 3.5 the concentration changes for the ME condition of the five different ROIs are presented in one plot in order to show a direct comparison between the ROIs. The latency difference between $ME_{20\%}$ and $ME_{40\%}$, that was described in chapter 3.1, is clearly recognizable in these graphs.

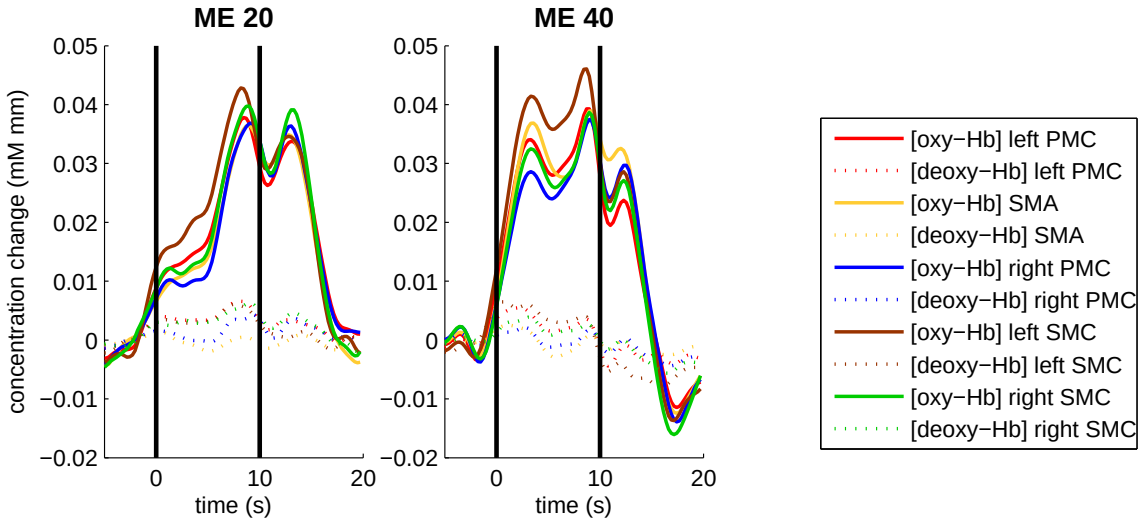

Figure 3.5: Comparison of [oxy-Hb] (solid lines) and [deoxy-Hb] (dotted lines) for the five ROIs for $ME_{20\%}$ and $ME_{40\%}$

As we can see in figure 3.6, for $MI_{20\%}$, the [oxy-Hb] in the supplementary motor area (SMA) is the highest from second 0 to second 10. Although [oxy-Hb] increases later in the right SMC than in any other ROI, it has the highest maximum value.

As in case of $MI_{20\%}$, SMA yields the highest values of [oxy-Hb] within the marked 10 s period for $MI_{40\%}$. However, the maximum values of [oxy-Hb] can be observed in the left PMC, and not in the right SMC, as it was the case for $MI_{20\%}$.

The 2x2x5 ANOVA revealed no significant results regarding the differences between the ROIs for ME or MI, which is represented by the *ROI* factor of the ANOVA. This can be seen in table 3.1 for oxy-Hb ($F(4,48)=0.3556$, $p=0.8389$) and for deoxy-Hb ($F(4,48)=0.7465$, $p=0.5652$).

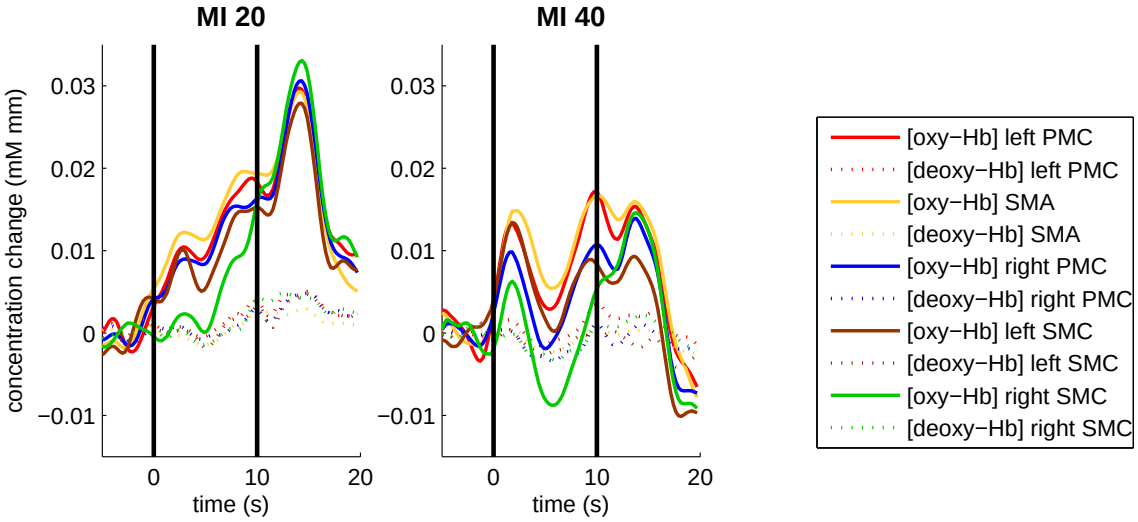

Figure 3.6: Comparison of [oxy-Hb] (solid lines) and [deoxy-Hb] (dotted lines) for the five ROIs for $MI_{20\%}$ and $MI_{40\%}$

3.5 Topographic distribution

The figures 3.7, 3.9, 3.11 and 3.13 illustrate topographic maps of grand average activation over 13 subjects for four different time frames for [oxy-Hb] and [deoxy-Hb] for each condition. The enlarged topographic maps of the time frames with the highest [oxy-Hb] values for every task are illustrated in the figures 3.8, 3.10, 3.12 and 3.14. In these topographic maps, the five ROIs are highlighted.

In the topographic maps for $ME_{20\%}$ and $ME_{40\%}$, the activation of the motor cortex is highest during the second time frame (t=5-10s) for both forces. Besides the activation of the motor cortex, an activation of the visual cortex is visible from second 5 to second 15 for $ME_{20\%}$ and second 0 to second 10 for $ME_{40\%}$. Additionally, the activation in the left hemisphere of the motor cortex is higher than in the right hemisphere, indicating a lateralization effect. However, the results of the paired-samples t-test do not confirm this observation, neither for $ME_{20\%}$ nor $ME_{40\%}$ (see table 3.4).

Table 3.4: Results of the paired-samples t-tests comparing right and left SMC for ME

	oxy-Hb		**deoxy-Hb**	
$\mathbf{ME_{20\%}}$	t(12)=-0.7417	p=0.4725	t(12)=-0.5382	p=0.6003
$\mathbf{ME_{40\%}}$	t(12)=1.0612	p=0.3095	t(12)=-0.6582	p=0.5229

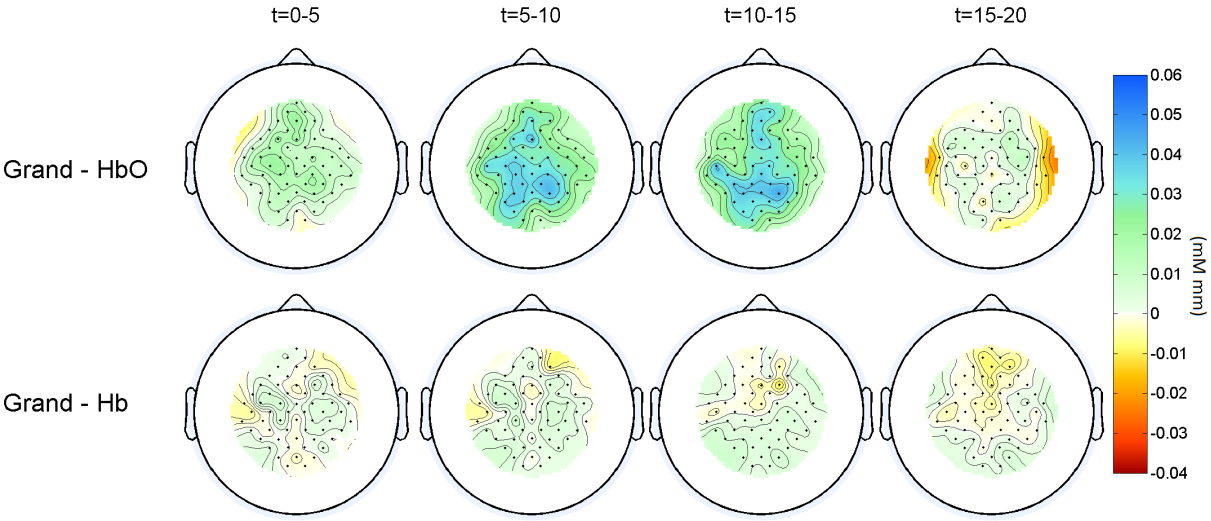

Figure 3.7: Topographic maps of [oxy-Hb] (upper panel) and [deoxy-Hb] (lower panel) for $ME_{20\%}$

As already mentioned, during $ME_{20\%}$, the activation in the left hemisphere of the motor cortex is higher than in the right hemisphere of the motor cortex. This can be seen in the enlarged topographic map of [oxy-Hb] in figure 3.8.

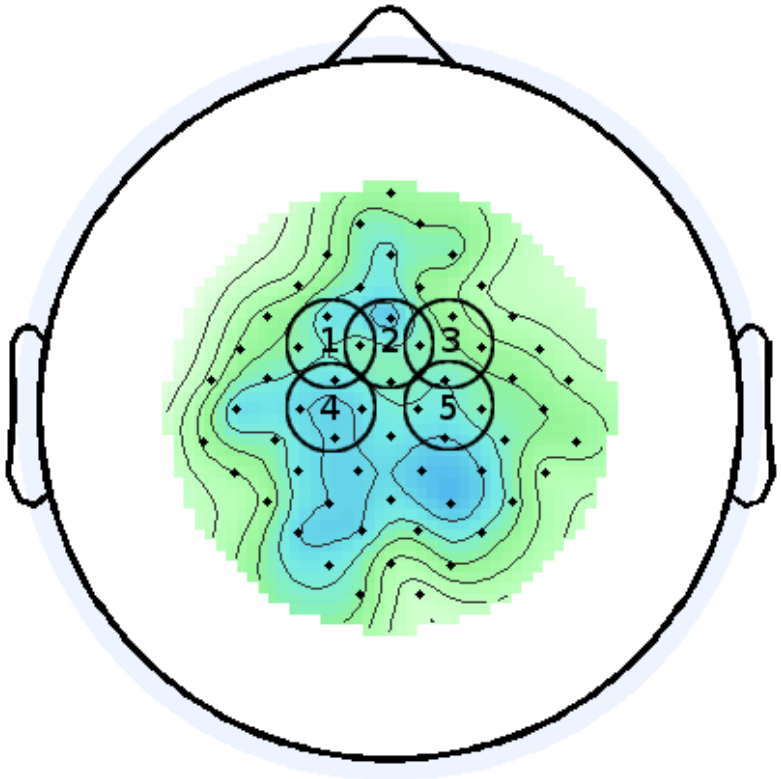

Figure 3.8: Enlarged topographic map of [oxy-Hb] for $ME_{20\%}$ (t=5-10s)

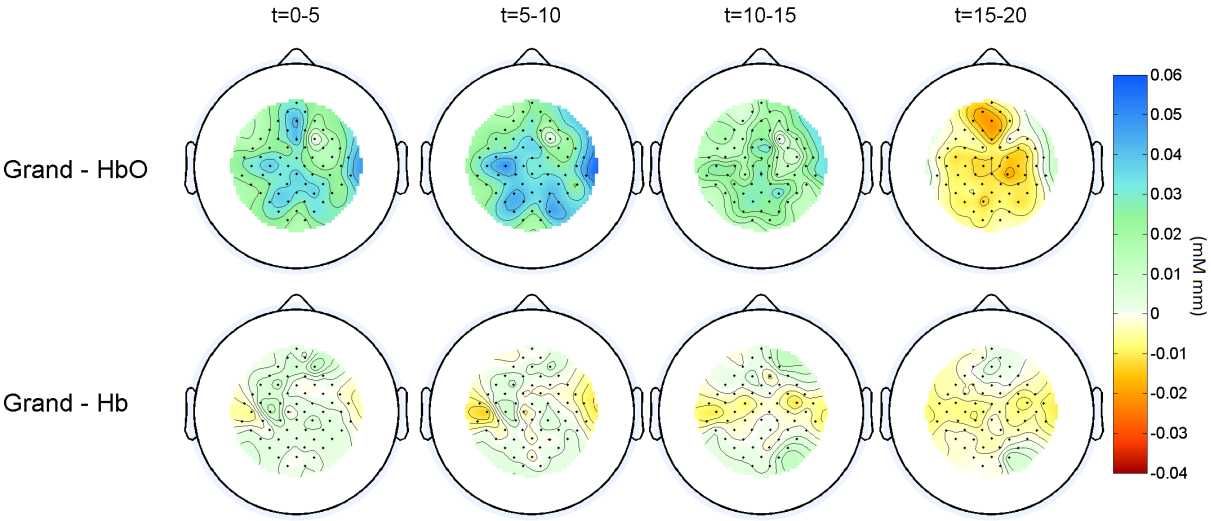

Figure 3.9: Topographic maps of [oxy-Hb] (upper panel) and [deoxy-Hb] (lower panel) for $ME_{40\%}$

In the enlarged topographic map of [oxy-Hb] for $ME_{40\%}$ in figure 3.10, a lateralization effect is again observable.

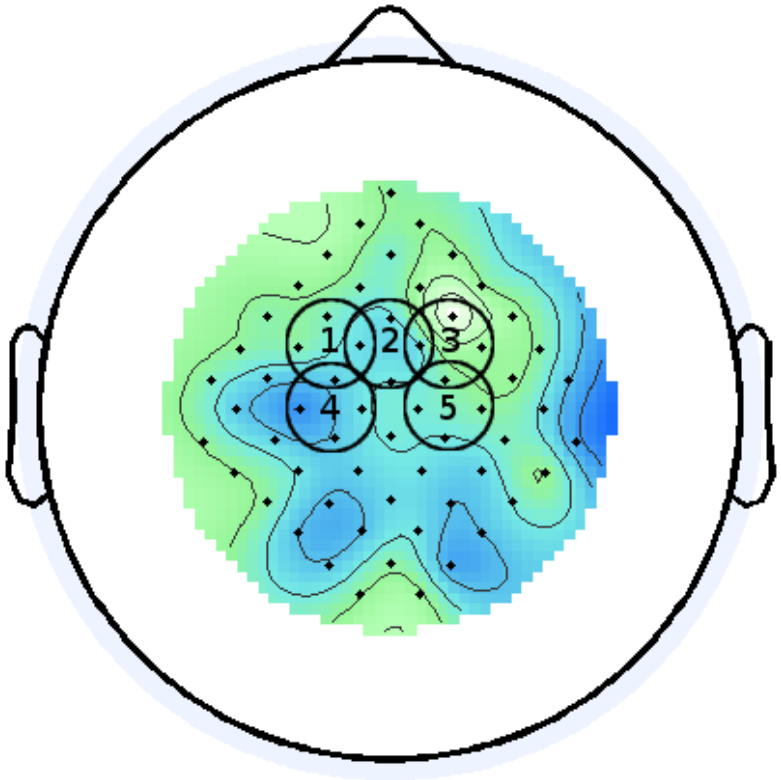

Figure 3.10: Enlarged topographic map of [oxy-Hb] for $ME_{40\%}$ (t=5-10s)

The topographic maps for $MI_{20\%}$ display a different activation pattern. The highest activation can be observed in the third time frame, between second 10 and second 15, at the visual cortex. An additional activation pattern can be observed in the prefrontal area. The motor cortex shows only a slight activation, without an observable lateralization.
For $MI_{40\%}$ there is even less activation observable. From second 5 and second 10, the concentration of oxy-Hb on the right hemisphere of the motor cortex is negative. The only visible activation can be observed in the visual cortex in the time frame from second 10 to 15.

The results of the performed paired-samples t-tests reveal no significant result regarding differences between left SMC and right SMC for MI. (see table 3.5)

Table 3.5: Results of the paired-samples t-tests comparing right and left SMC for MI

	oxy-Hb		**deoxy-Hb**	
$\mathbf{MI}_{20\%}$	t(12)=-1.0388	p=0.3194	t(12)=-0.5942	p=0.5634
$\mathbf{MI}_{40\%}$	t(12)=-0.9387	p=0.3664	t(12)=-0.5091	p=0.6199

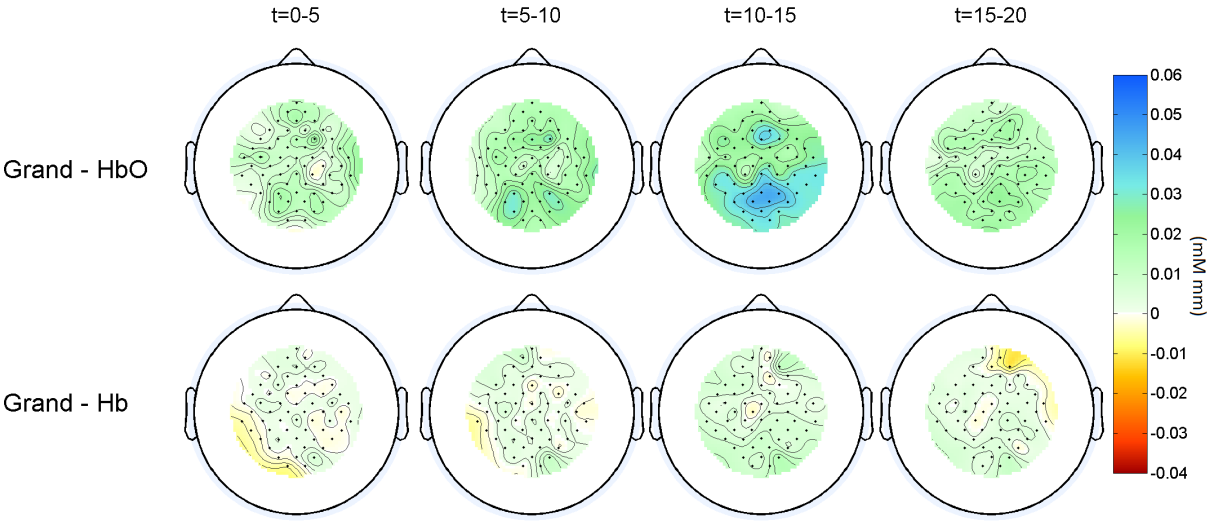

Figure 3.11: Topographic maps of [oxy-Hb] (upper panel) and [deoxy-Hb] (lower panel) for $MI_{20\%}$

As mentioned before, the highest activation during $MI_{20\%}$ is above the prefrontal area and the visual cortex, visible in the enlarged topographic map in figure 3.12.

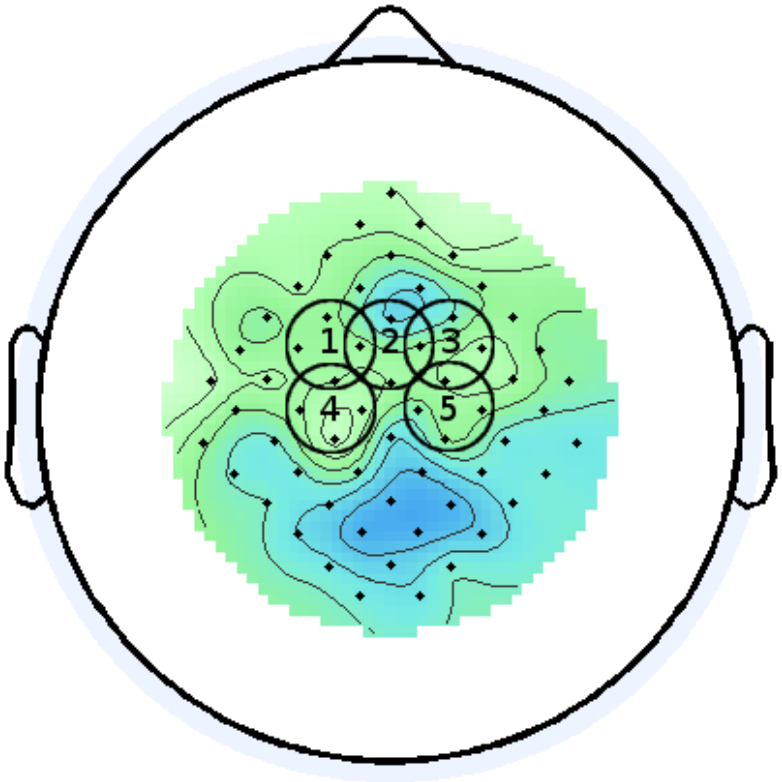

Figure 3.12: Enlarged topographic map of [oxy-Hb] for $MI_{20\%}$ (t=10-15s)

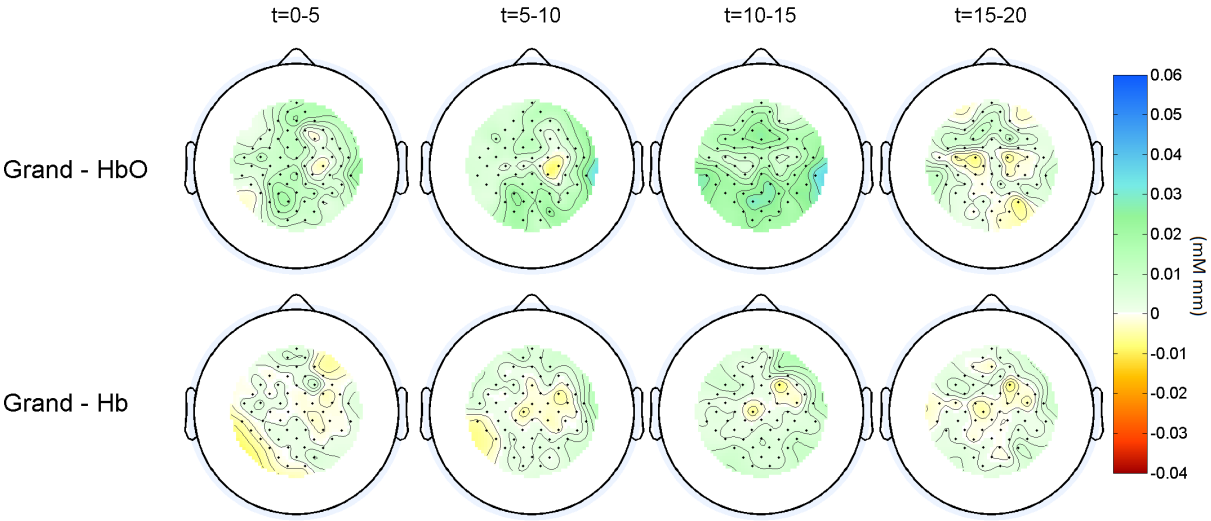

Figure 3.13: Topographic maps of [oxy-Hb] (upper panel) and [deoxy-Hb] (lower panel) for $MI_{40\%}$

For $MI_{40\%}$, the enlarged topographic map in figure 3.14 only reveals an activation above the visual cortex.

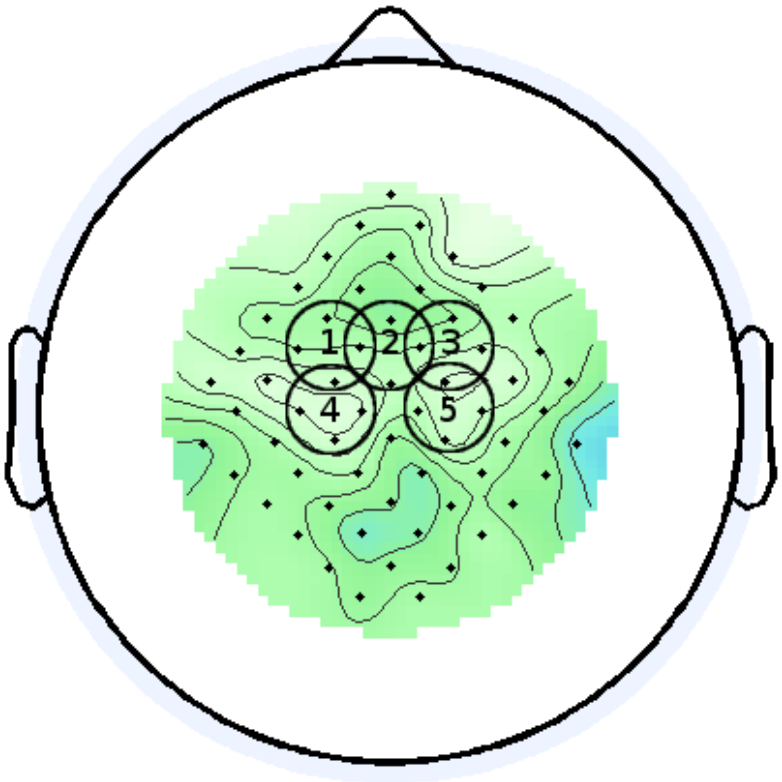

Figure 3.14: Enlarged topographic map of [oxy-Hb] for $MI_{40\%}$ (t=10-15s)

4 Discussion

In the following sections, the obtained results are discussed and the limitations of this study are mentioned.

4.1 Differences in the amount of activation for MI and ME

The examination of possible differences in the activation patterns of ME and MI was done with a 2x2x5 ANOVA. The results of this test, presented in table 3.1, clearly stated that there is a significant main effect of the factor *Task*, i.e. ME and MI, with a p-value of 0.00048 ($F(1,12)=22.45$). A closer look revealed, that the difference between the two tasks was in form of a higher activation for ME than for MI, as can be seen in figure 3.1. The respective means also confirmed, that the concentration change of oxy-Hb during the ME condition was higher than during MI condition, representing a higher amount of activation.

This is in line with previous studies claiming a higher activation for ME than MI. For example, *Wriessnegger et al.* also examined the differences between movement execution and imagery, with a focus on spatio-temporal characteristics. Their results of an ANOVA on the variable peak maxima also yielded a significant main effect of the factor *Task (MI, ME)*, meaning higher peak maxima for ME than for MI can be expected. [42]

The difference in the amount of activation can be explained by the more complex cognitive requirements of imagination. Although similar cortical regions are activated, the more complex nature of MI may lead to the lower activation for MI compared to ME. [19, 42]

4.2 Motor execution

Differences between $ME_{20\%}$ and $ME_{40\%}$ are observable in figure 3.2, where the concentration changes for the five ROIs are illustrated for the ME condition. In three ROIs, namely left SMC, left PMC and SMA, the maximum values of [oxy-Hb] for $ME_{40\%}$ were slightly higher than that of $ME_{20\%}$. Within the same ROIs, [oxy-Hb] showed the most prominent increase during $ME_{40\%}$ as illustrated in figure 3.5. The different time courses depending on the ROI will be further described in the sub chapter 4.5.

Although the topographic maps indicated a difference in the amount of activation between $ME_{20\%}$ and $ME_{40\%}$, the statistical analysis of the impact of using different grip strengths during motor execution tasks revealed no significant results. Neither the factor *Force* of the 2x2x5 ANOVA (see table 3.1), nor the further investigation of the different ROIs with a paired-samples t-test (see table 3.2) confirmed any differences regarding the amount of activation.

Besides the differences in the amount of activation, different time courses of [oxy-Hb] for $ME_{20\%}$ and $ME_{40\%}$ were evident in figure 3.2, independent of the ROI. For $ME_{40\%}$, [oxy-Hb] rose constantly during the first few seconds (-2 - 3 s), whereas [oxy-Hb] for $ME_{20\%}$ showed a slower increase, and therefore reached its first peak at a later point in time. Additionally, it was levelled out later. There is no evident reason for this latency difference between $ME_{20\%}$ and $ME_{40\%}$ available.

Since to the best of my knowledge, no studies have been done investigating differences in brain activation with different forces, there is no comparative data available. Further measurements are necessary to gain more insights in brain activity during MI and ME with different forces.

4.3 Motor imagery

As already mentioned, the 2x2x5 ANOVA revealed no significant main effect for the factor *Force*. However, a closer look on the different plots for the MI condition in figure 3.3 suggests, that the force may have some influence on the haemodynamic response. According to this illustration, the mean concentration changes of oxy-Hb were lower for the $MI_{40\%}$ task than for the $MI_{20\%}$ in every ROI. This was also confirmed by the calculation of the average of the maximum values for $MI_{20\%}$ and $MI_{40\%}$, which exhibited a difference of approximately 0.01 mM mm.

According to the paired-samples t-test and the calculated averages of the maximum values for $MI_{20\%}$ and $MI_{40\%}$, higher values for the concentration change for $MI_{20\%}$ can be expected in the right PMC (ROI 3, see table 3.3). For the other ROIs, the t-test revealed no significant results.

As already observed for $ME_{40\%}$, [oxy-Hb] for $MI_{40\%}$ increased faster during the first few seconds than [oxy-Hb] for $MI_{20\%}$ (see figure 3.3). After those few seconds, the values for [oxy-Hb] for $MI_{40\%}$ dropped again, until a local minima approximately at second 5 occurred in every ROI. Although the time course for [oxy-Hb] for $MI_{40\%}$ also displays small decreases, it exceeded $MI_{40\%}$ approximately from second 3 until the rest of the activation period.

The vividness of MI depends on the experience in performing the task, the content of the task and the individual's ability for imagery [17]. The experience in performing the task can be considered as given, because it can be expected that the subjects performed hand grips in their everyday life. Additionally, every subject had to perform several hand grip exercises prior to the measurement as a training. A possible variability lies within each subjects' ability for motor imagery. An additional difficulty was the imagery of a hand grip with the 2 different strength levels (20% and 40%). This could explain the observed differences between $MI_{20\%}$ and $MI_{40\%}$. However, it does not seem likely, that the capability of a subject to vividly perform MI is dependent on the imagined grip strength. However, this does not explain the observed differences between $MI_{20\%}$ and $MI_{40\%}$, because the ability of a person to vividly perform MI is independent of the imagined grip strength.

Due to the fact that no studies on MI with different grip strengths were found, no comparison of the recent findings with other publications is possible.

4.4 Latency differences between MI and ME

In figure 3.4, the different time courses for [oxy-Hb] and [deoxy-Hb] for ME and MI for each of the five ROIs, a peak latency difference for [oxy-Hb] between ME and MI is shown. This peak latency is visible in every ROI. This was also confirmed by the calculation of the average peak time over all subjects for [oxy-Hb], which is 3 seconds earlier for ME than for MI.

For example, *Wriessnegger et al.*, who employed a tapping task with MI and ME, reported a delayed oxygenation response in the imagery task as well. They suggested the higher complexity of the imagery task compared to motor execution as a possible reason for this latency difference. [42]

4.5 Differences between ROIs

In figure 3.5, the concentration changes for $ME_{20\%}$ and $ME_{40\%}$ are displayed, comparing each of the five different ROIs. For both $ME_{20\%}$ and $ME_{40\%}$, left SMC showed the highest values with the fastest response for both conditions. For $ME_{20\%}$, the ROI with the second highest activation was the right SMC, and for $ME_{40\%}$ it was the SMA. After that, no clear distinction between the ROIs is possible, since the three remaining ROIs are approximately in the same range.

A possible reason, why the left SMC was higher for both conditions than the left PMC, is the difference in the role of these brain regions. It is commonly known that the PMC is involved in the planning of movements, whereas the SMC is responsible for movement execution [27]. Therefore it seems reasonable, that this ROI showed the highest activation.

Figure 3.6 depicts the concentration changes for the five different ROIs for the motor imagery condition. The SMA showed the fastest increase and the highest amplitudes of [oxy-Hb] for both $MI_{20\%}$ and $MI_{40\%}$ at first. This high activation of the SMA is consistent with previous studies, who found, that the SMA plays a major role in MI. [17]

The conducted 2x2x5 ANOVA did not confirm any differences between the ROIs, as can be seen in table 3.1 for the factor *ROI*.

The results are in line with a study by *Wriessnegger et al.*, who compared MI and ME in the prefrontal cortex, the primary motor cortex and somatosensory regions and also found differences in the [oxy-Hb] increases between the different ROIs. For ME, they found a high activation in the primarily motor areas, whereas for motor imagery, the activation was equally distributed over frontal, central and posterior sites. [42]

Also, *Iso et al.*, who investigated the haemodynamic response to a tapping task, reported a particularly high activation of [oxy-Hb] in the SMC of the contralateral hand during ME. Additionally, their study revealed lower activation of primary motor areas during imagery than during execution. SMA and PMC, however, were activated to a similar extent during ME and MI. [17] Since the SMA is involved in movement planning [22], this high activation during MI seems reasonable, but was not present in this work, where the observed activation for MI in SMA is definitely lower than for ME (see figure 3.4). As already described in subsection 4.1, this lower activation for MI can be explained by the more complex cognitive requirements of imagination compared to ME.

4.6 Topographic distribution

As described, the topographic maps indicated possible lateralization effect for ME. Such lateralization effects during motor execution and motor imagery were reported by different studies. For example, *Suto et al.* found contralateral activation during a right finger tapping task. [38] *Horovitz and Gore* also detected higher activation over the motor cortex of the contralateral side as a result of finger tapping. [16] Another study employing a tapping sequence done by *Iso et al.* depicted an increase of [oxy-Hb] in the contralateral somatosensory motor cortex during ME. [17]

On the other hand, bilateral activation was also observed by a variety of studies. For example during a combined NIRS-fMRI study with a unilateral finger opposition task done by *Kleinschmidt et al.*, [oxy-Hb] displayed no lateralization. [24] Also, *Wriessnegger et al.* detected bilateral activation during both motor imagery and motor execution, except for left hand motor execution, which showed a contralateral activation. [42]

In the present work, a contralateral activation for the motor execution condition was found . In the enlarged topographic map for [oxy-Hb] for $ME_{40\%}$ in figure 3.10, a lateralization is clearly visible. For $ME_{40\%}$, this lateralization is not as prominent, but also observable, as shown in figure 3.8.

As already described, [oxy-Hb] for both $ME_{20\%}$ and $ME_{40\%}$ exhibits the highest amplitudes in the left SMC, displayed in figure 3.5. However, the conducted paired-samples t-test did not confirm differences in the amount of activation between left and right SMC for ME (see table 3.4). Also, for MI, no lateralization effect can be observed, neither for $MI_{20\%}$ nor $MI_{40\%}$ (see figures 3.12 and 3.14).

4.7 The concentration change of deoxy-Hb

The time course for [deoxy-Hb] did not follow the typical temporal pattern, that was described in chapter 1.3. According to *Leff et al.*, [deoxy-Hb] slowly decreases during activation of a brain region. Neither for MI nor ME, this pattern can be observed. Instead of a clear increase or decrease, no obvious tendency is noticeable, instead it is fluctuating during the whole time frame. In a study by *Iso et al.*, the time courses of [deoxy-Hb] for both ME and MI showed similar patterns, as can be seen in figure 4.1 for the ME with the left hand (red lines) [17]. Unfortunately, they did not explain this phenomenon.

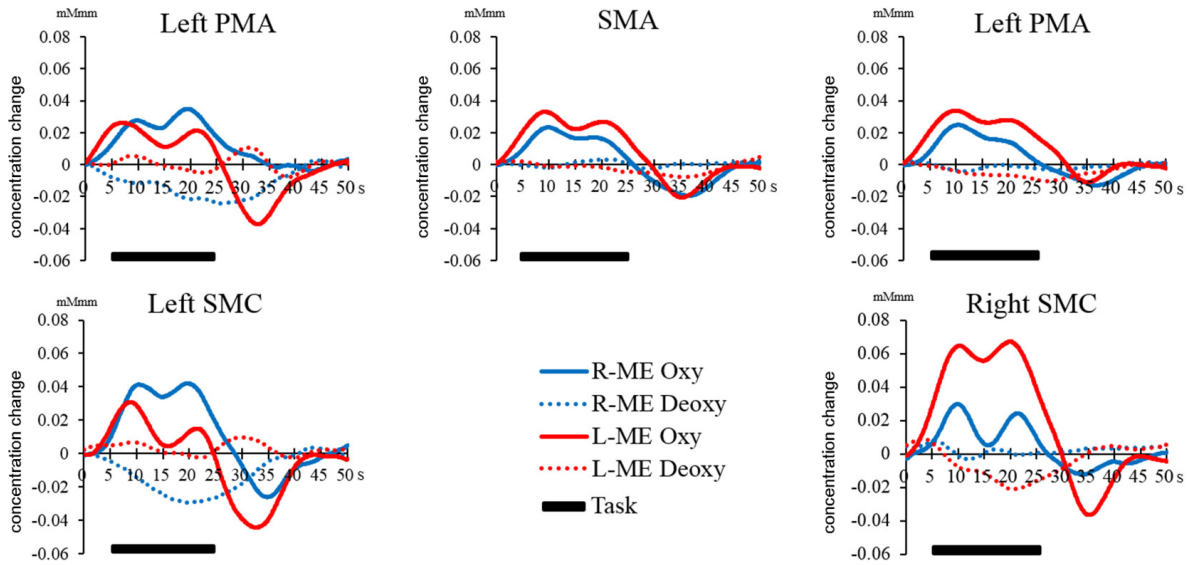

Figure 4.1: [oxy-Hb] (solid lines) and [deoxy-Hb] (dotted lines) in the regions of interest for ME with left hand (L-ME) and with right hand (R-ME) (modified from [17])

4.8 Limitations and recommendations for further studies

One recommendation for further studies concerns the timing of the paradigm. During this study, the intertrial interval was set to 10 to 14 s, which is consistent with a recommendation by *Leff et al.* [27]. For figure 4.2, the earliest possible point for the start of the next trial was marked in the measured concentration changes for $MI_{20\%}$. As can be seen, the haemodynamic response did not return to baseline before the next trial started. This is also true for the other conditions.

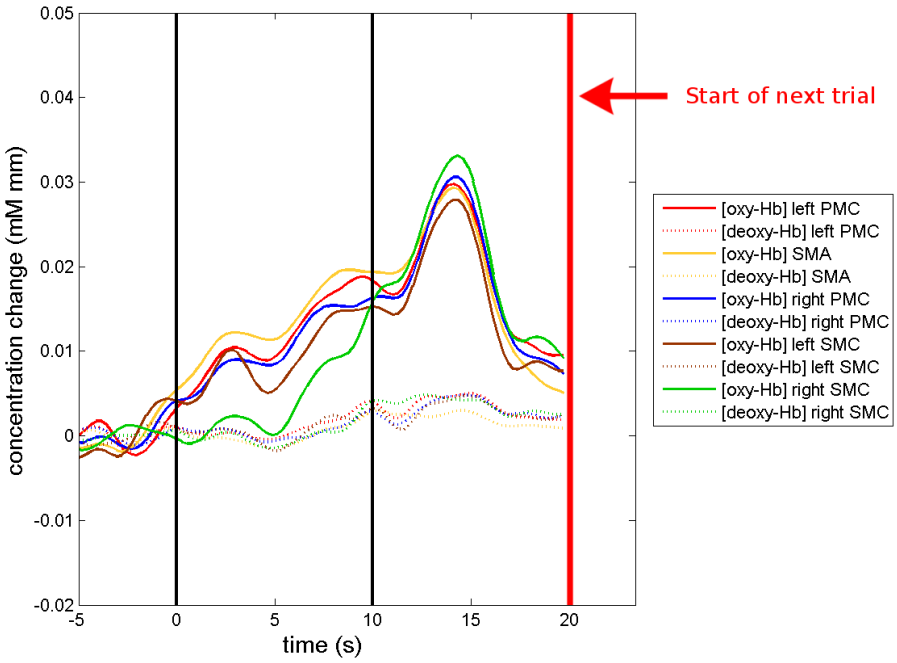

Figure 4.2: [oxy-Hb] (solid lines) and [deoxy-Hb] (dotted lines) for $MI_{20\%}$ with a red line indicating a possible start point of the next trial

Additionally, testing the subjects ability of mental imagery is suggested. Possible ways to do so would habe been in form of the Kinesthetic and Visual Imagery Questionnaire-20 (KVIQ-20) [29] or the Movement Imagery Questionnaire-Revised Second Version (MIQ-RS) [11]. These questionnaires would provide subjective evaluation of the vividness of MI.

Another limitation of this study is the rather small sample size (N=13). Although some statistically significant results were found, more measurements are necessary to confirm these findings.

A possible improvement for the MI condition would be the usage of real neurofeedback instead of sham feedback. *Mihara et al.* found that real neurofeedback led to higher activation in the premotor cortex and higher scores in self-assessments. [30]

One last limitation of this study was the lacking of an EMG recording concurrently with the MI condition, in order to exclude muscular activation.

5 Conclusion

The aim of this thesis was to investigate the haemodynamic response for MI and ME with a hand grip task using two different grip strengths. One of the major results was the activation differences between ME and MI, independent of the grip strength. The amount of activation was found to be lower for MI than for ME. A possible explanation for this lies in the higher cognitive requirements for MI. Additionally, a latency difference between ME and MI was observable. MI showed an oxygenation peak latency difference of 3 s compared to ME for the 13 measured subjects.

Differences in the haemodynamic response for the two used grip strengths were present. For ME, an oxygenation latency difference between the two grip strengths was found. During the MI condition, no such latency difference could be observed. Only for one ROI, the statistical tests revealed a significant result, stating, that higher [oxy-Hb] peaks can be expected for $MI_{20\%}$ than for $MI_{40\%}$.

Although the conducted ANOVA yielded no significant result on the factor *ROI*, the investigation of possible differences between the ROIs will be nonetheless interesting for future studies. According to the averaged concentration changes, the left SMC showed the highest values and the fastest response for both $ME_{20\%}$ and $ME_{40\%}$ for [oxy-Hb]. This seems reasonable, since the SMC plays a major role during the execution of a movement.

Concluding, the investigation of MI and ME with a hand grip task using two different grip strengths showed some new results. However, further investigations are necessary in order to allow statistically significant statements.

References

[1] Annett J. Motor imagery: perception or action? *Neuropsychologia* 33(11):1395–1417 (1995)

[2] Bauernfeind G. Using Functional Near-Infrared Spectroscopy (fNIRS) for Optical Brain-Computer Interface (oBCI) Applications. *PhD thesis* (2012)

[3] Bauernfeind G, Wriessnegger S C, Daly I, Müller-Putz G R. Separating heart and brain: on the reduction of physiological noise from multichannel functional near-infrared spectroscopy (fNIRS) signals. *Journal of neural engineering* 11(5):056010 (2014)

[4] Boden S, Obrig H, Köhncke C, Benav H, Koch S P, Steinbrink J. The oxygenation response to functional stimulation: Is there a physiological meaning to the lag between parameters? *NeuroImage* 36(1):100–107 (2007)

[5] Calautti C, Baron J C. Functional Neuroimaging Studies of Motor Recovery After Stroke in Adults A Review. *Stroke* 34(6):1553–1566 (2003)

[6] Cope M. The Application Of Near Infrared Spectroscopy To Non Invasive Monitoring Of Cerebral Oxygenation In The Newborn Infant. *PhD thesis* page 342 (1991)

[7] Coyle S M, Ward T E, Markham C M, Ward E, Markham C M. Brain-computer interface using a simplified functional near-infrared spectroscopy system. *Journal of neural engineering* 4(3):219–26 (2007)

[8] Elwell C E, Springett R, Hillman E, Delpy D T. Oscillations in cerebral haemodynamics. Implications for functional activation studies. *Advances in experimental medicine and biology* 471:57–65 (1999)

[9] Ferrari M, Quaresima V. A brief review on the history of human functional near-infrared spectroscopy (fNIRS) development and fields of application. *NeuroImage* 63(2):921–935 (2012)

[10] Franceschini M A, Fantini S, Thompson J H, Culver J P, Boas D A. Hemodynamic evoked response of the sensorimotor cortex measured noninvasively with near-infrared optical imaging. *Psychophysiology* 40(4):548–560 (2003)

[11] Gregg M, Hall C, Butler A. The MIQ-RS: A suitable Option for examining movement imagery ability. *Evidence-based Complementary and Alternative Medicine* 7(2):249–257 (2010)

[12] Griebler R, Anzenberger J, Eisenmann A. Herz-Kreislauf-Erkrankungen in Österreich. *Bundesministerium für Gesundheit* (2014)

[13] Hatakenaka M, Miyai I, Mihara M, Sakoda S, Kubota K. Frontal regions involved in learning of motor skill-A functional NIRS study. *NeuroImage* 34(1):109–116 (2007)

[14] Hendricks H T, Van Limbeek J, Geurts A C, Zwarts M J. Motor recovery after stroke: A systematic review of the literature. *Archives of Physical Medicine and Rehabilitation* 83(11):1629–1637 (2002)

[15] Holper L, Wolf M. Motor imagery in response to fake feedback measured by functional near-infrared spectroscopy. *NeuroImage* 50(1):190–197 (2010)

[16] Horovitz S, Gore J. Studies of the sensitivity of near infrared spectroscopy to detect changes in levels of brain activation due to manipulations of motor tasks. *Proceedings of the 25th Annual International Conference of the IEEE Engineering in Medicine and Biology Society (IEEE Cat No03CH37439)* pages 1106–1108 (2003)

[17] Iso N, Moriuchi T, Sagari A, Kitajima E, Iso F, Tanaka K, Kikuchi Y, Tabira T, Higashi T. Monitoring Local Regional Hemodynamic Signal Changes during Motor Execution and Motor Imagery Using Near-Infrared Spectroscopy. *Frontiers in Physiology* 6(416) (2016)

[18] Jeannerod M. The representing brain: Neural correlates of motor intention and imagery. *Behavioral and Brain Sciences* 17(02):187 (1994)

[19] Jeannerod M, Decety J. Mental motor imagery: a window into the representational stages of action. *Current Opinion in Neurobiology* 5(6):727–732 (1995)

[20] Jöbsis F F. Noninvasive, Infrared Monitoring of Cerebral and Myocardial Oxygen Sufficiency and Circulatory Parameters. *Science* 198(4323):1264–1267 (1977)

[21] Kaiser V, Daly I, Pichiorri F, Mattia D, Müller-Putz G R, Neuper C. Relationship between electrical brain responses to motor imagery and motor impairment in stroke. *Stroke* 43(10):2735–2740 (2012)

[22] Kasess C H, Windischberger C, Cunnington R, Lanzenberger R, Pezawas L, Moser E. The suppressive influence of SMA on M1 in motor imagery revealed by fMRI and dynamic causal modeling. *NeuroImage* 40(2):828–837 (2008)

[23] Kato H, Izumiyama M, Koizumi H, Takahashi A, Itoyama Y. Near-infrared spectroscopic topography as a tool to monitor motor reorganization after hemiparetic stroke: A comparison with functional MRI. *Stroke* 33(8):2032–2036 (2002)

[24] Kleinschmidt A, Obrig H, Requardt M, Merboldt K d, Dirnagl U, Villringer A, Frahm J. Simultaneous Recording of Cerebral Blood Oxygenation Changes During Human Brain Activation by Magnetic Resonance Imaging and Near-Infrared Spectroscopy. *Journal of Cerebral Blood Flow and Metabolism* 16(5):817–826 (1996)

[25] Langhorne P, Bernhardt J, Kwakkel G. Stroke rehabilitation. *The Lancet* 377(9778):1693–1702 (2011)

[26] Langhorne P, Coupar F, Pollock A. Motor recovery after stroke: a systematic review. *The Lancet Neurology* 8(8):741–754 (2009)

[27] Leff D R, Orihuela-Espina F, Elwell C E, Athanasiou T, Delpy D T, Darzi A W, Yang G Z. Assessment of the cerebral cortex during motor task behaviours in adults: A systematic review of functional near infrared spectroscopy (fNIRS) studies. *NeuroImage* 54(4):2922–2936 (2011)

[28] Malonek D, Grinvald A. Interactions between electrical activity and cortical microcirculation revealed by imaging spectroscopy. *Science* 272:551–554 (1996)

[29] Malouin F, Richards C L, Jackson P L, Lafleur M F, Durand A, Doyon J. The Kinesthetic and Visual Imagery Questionnaire (KVIQ) for assessing motor imagery in persons with physical disabilities: a reliability and construct validity study. *Journal of neurologic physical therapy : JNPT* 31(1):20–29 (2007)

[30] Mihara M, Miyai I, Hattori N, Hatakenaka M, Yagura H, Kawano T, Okibayashi M, Danjo N, Ishikawa A, Inoue Y, Kubota K. Neurofeedback using real-time near-infrared spectroscopy enhances motor imagery related cortical activation. *PLoS ONE* 7(3) (2012)

[31] Miyai I, Yagura H, Hatakenaka M, Oda I, Konishi I, Kubota K. Longitudinal Optical Imaging Study for Locomotor Recovery after Stroke. *Stroke* 34(12):2866–2870 (2003)

[32] Neuper C, Scherer R, Reiner M, Pfurtscheller G. Imagery of motor actions: Differential effects of kinesthetic and visual-motor mode of imagery in single-trial EEG. *Cognitive Brain Research* 25(3):668–677 (2005)

[33] Obrig H, Villringer A. Beyond the visible - Imaging the human brain with light. *Journal of Cerebral Blood Flow and Metabolism* 23(1):1–18 (2003)

[34] Okada E, Firbank M, Schweiger M, Arridge S R, Cope M, Delpy D T. Theoretical and experimental investigation of near-infrared light propagation in a model of the adult head. *Applied optics* 36(1):21–31 (1997)

[35] Pfurtscheller G, Ortner R, Bauernfeind G, Linortner P, Neuper C. Does conscious intention to perform a motor act depend on slow cardiovascular rhythms? *Neuroscience Letters* 468(1):46–50 (2010)

[36] Pschyrembel W. *Pschyrembel klinisches Wörterbuch.* de Gruyter, 262 edition (2011)

[37] Schaechter J D. Motor rehabilitation and brain plasticity after hemiparetic stroke. *Progress in Neurobiology* 73(1):61–72 (2004)

[38] Suto T, Ito M, Uehara T, Ida I, Fukuda M, Mikuni M. Temporal characteristics of cerebral blood volume change in motor and somatosensory cortices revealed by multichannel near-infrared spectroscopy. *International Congress Series* 1232:383–388 (2002)

[39] Takeda K, Gomi Y, Imai I, Shimoda N, Hiwatari M, Kato H. Shift of motor activation areas during recovery from hemiparesis after cerebral infarction: A longitudinal study with near-infrared spectroscopy. *Neuroscience Research* 59(2):136–144 (2007)

[40] Ward N S, Brown M M, Thompson A J, Frackowiak R S J. Neural correlates of motor recovery after stroke: A longitudinal fMRI study. *Brain* 126(11):2476–2496 (2003)

[41] Wolf M, Wolf U, Toronov V, Michalos A, Paunescu L A, Choi J H, Gratton E. Different time evolution of oxyhemoglobin and deoxyhemoglobin concentration changes in the visual and motor cortices during functional stimulation: a near-infrared spectroscopy study. *Neuroimage* 16(3 Pt 1):704–712 (2002)

[42] Wriessnegger S C, Kurzmann J, Neuper C. Spatio-temporal differences in brain oxygenation between movement execution and imagery: A multichannel near-infrared spectroscopy study. *International Journal of Psychophysiology* 67(1):54–63 (2008)

[43] Yamashita Y, Maki A, Koizumi H. Near-infrared topographic measurement system: Imaging of absorbers localized in a scattering medium. *Review of Scientific Instruments* 67(3):730–732 (1996)

[44] Zimmermann-Schlatter A, Schuster C, Puhan M A, Siekierka E, Steurer J. Efficacy of motor imagery in post-stroke rehabilitation: a systematic review. *Journal of neuroengineering and rehabilitation* 5:8 (2008)